The Abdus Salam
International Centre for Theoretical Physics

United Nations
Educational, Scientific and
Cultural Organization

IAEA
International Atomic Energy Agency

2167-36

Advanced School on Direct and Inverse Problems of Seismology

27 September - 8 October, 2010

Structural models of the lithosphere-asthenosphere system in the Mediterranean and volcanic activity
Part 2

G.F. Panza

Dept. of Earth Sciences
University of Trieste/ICTP SAND Group
Trieste

Structural models of the lithosphere-asthenosphere system in the Mediterranean and volcanic activity

Giuliano F. Panza

Part 2

Advanced School on Direct and Inverse Problems of Seismology

ICTP - 27-9/9-10 2010

The lithosphere-asthenosphere system in the Mediterranean region and westward mantle flow


nasa

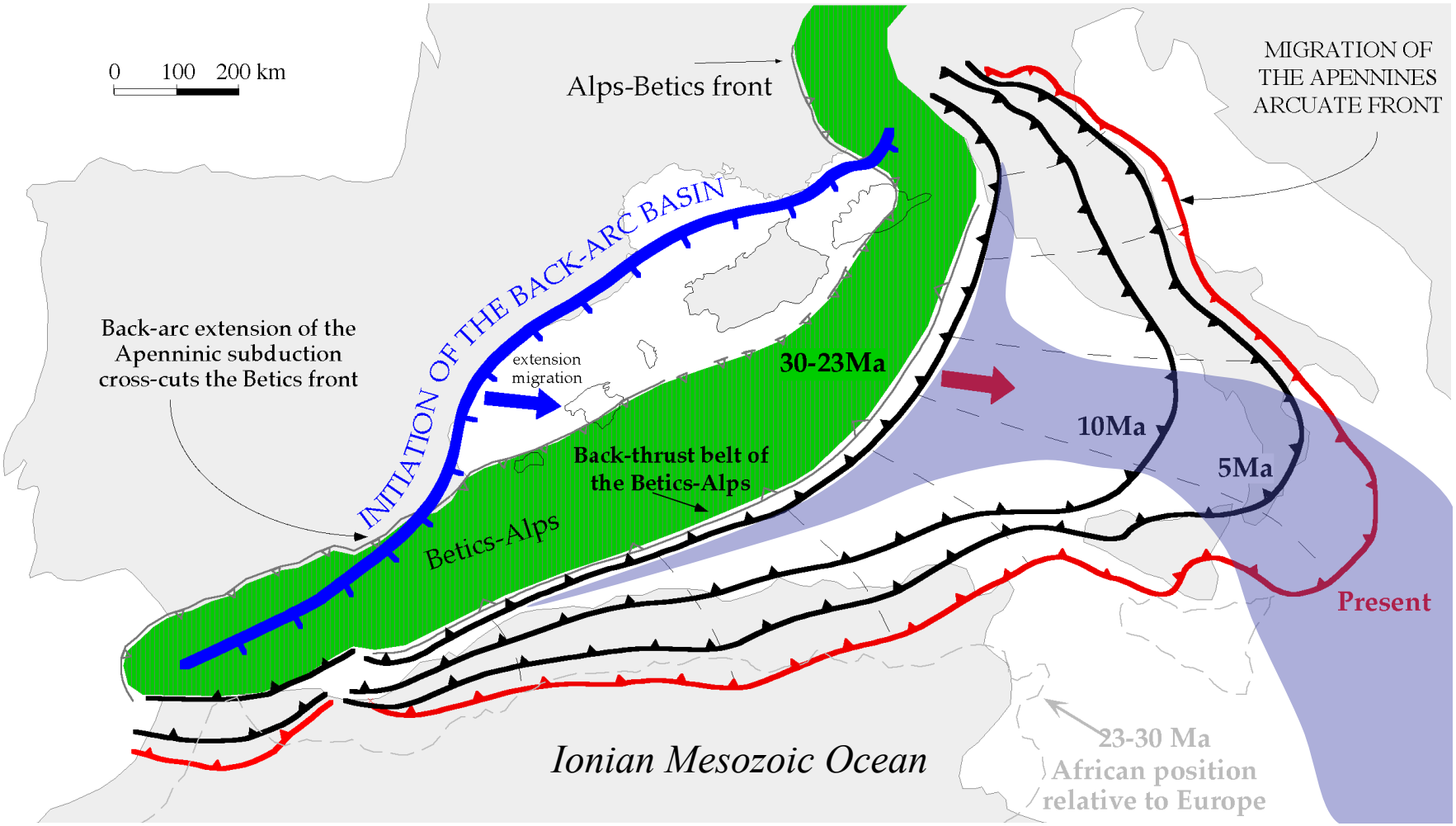

E-ward slab retreat
5 times faster than N-S convergence

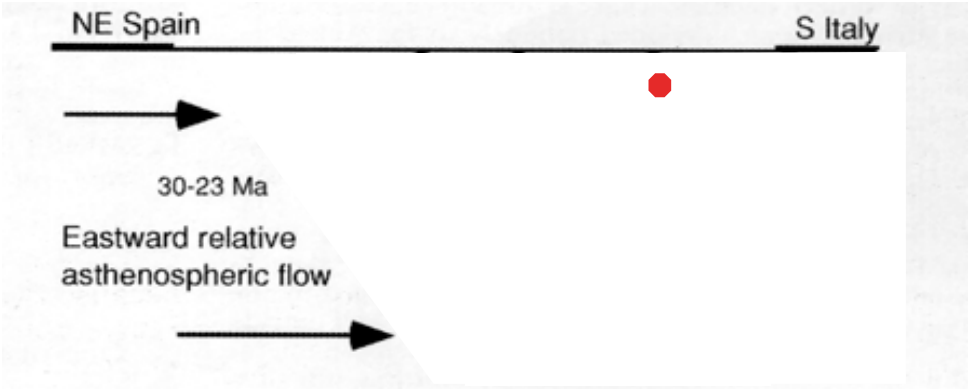

3D model of Vrancea; type B subduction

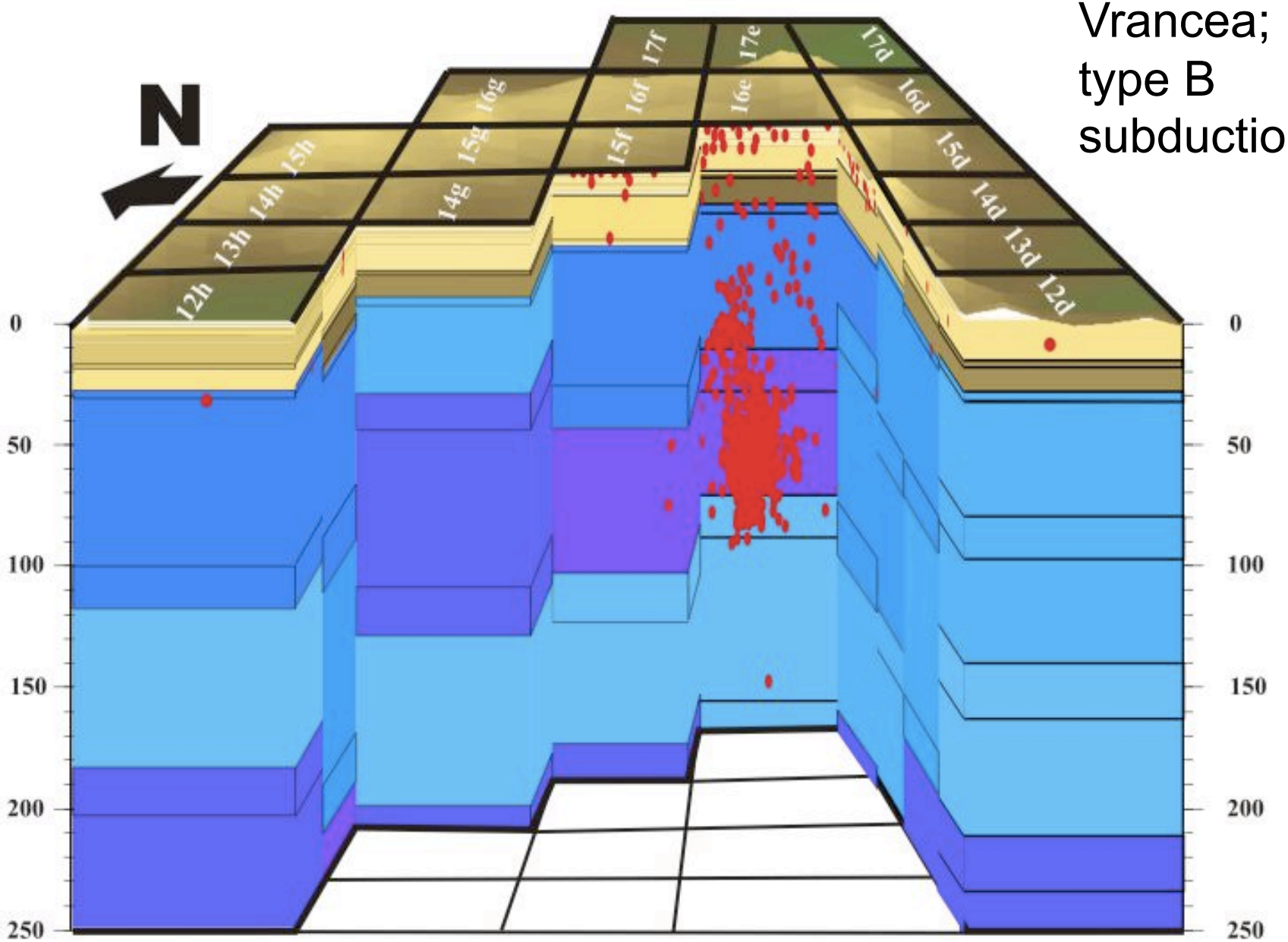

(Raykova and Panza, PEPI 2006)

Lithosphere-asthenosphere system along TRANSMED III

from non-linear inversion of surface-wave tomography data

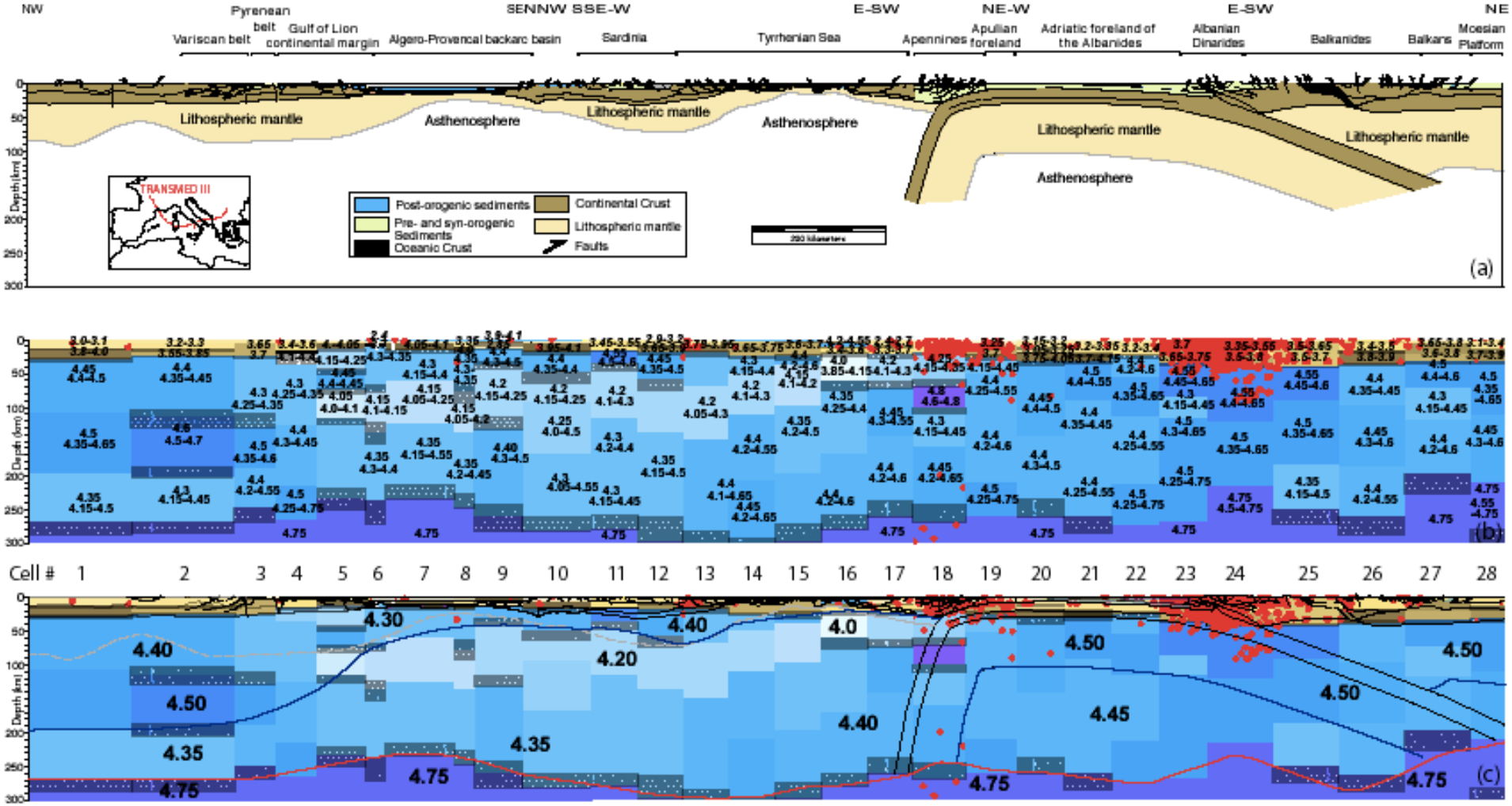

(Panza et al., EPSL, 2007)

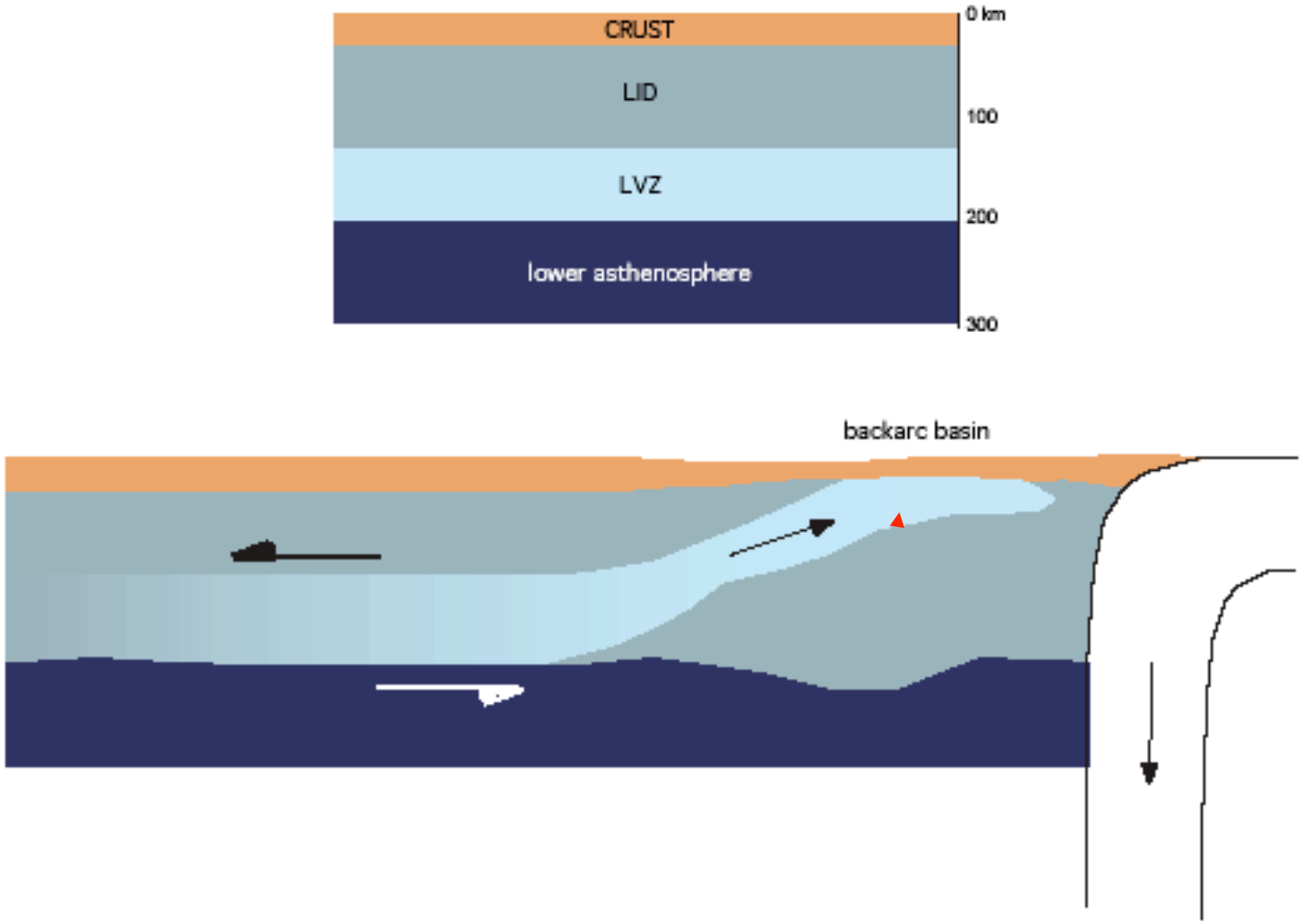

splash of mantle: volcanoes

(Panza et al., EPSL, 2007)

Cellular models, obtained from non-linear inversion of surface-wave tomography data, where active volcanoes are present

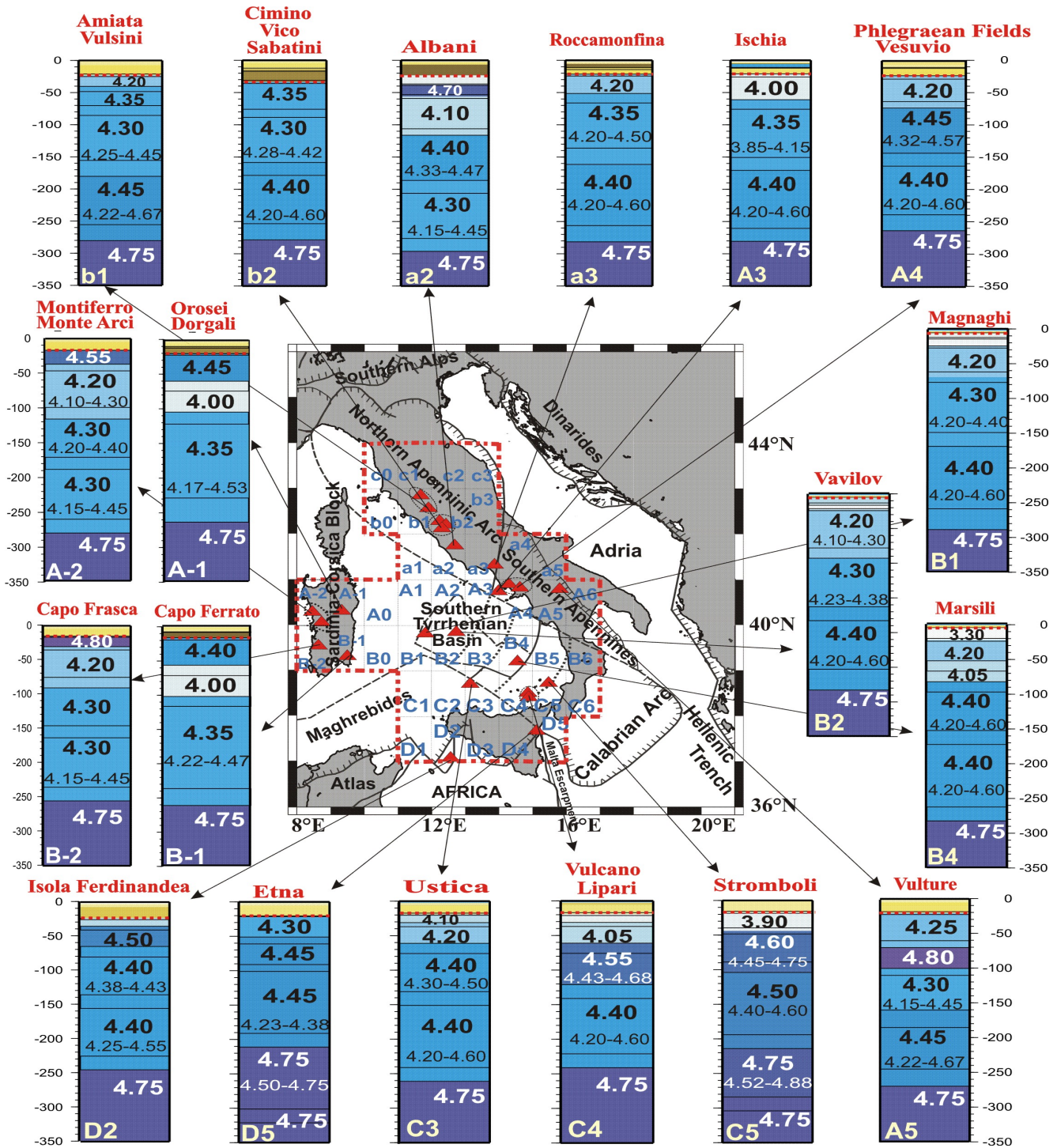

Plio-Quaternary magmatic provinces in Italy. Modified after Peccerillo and Panza (1999)

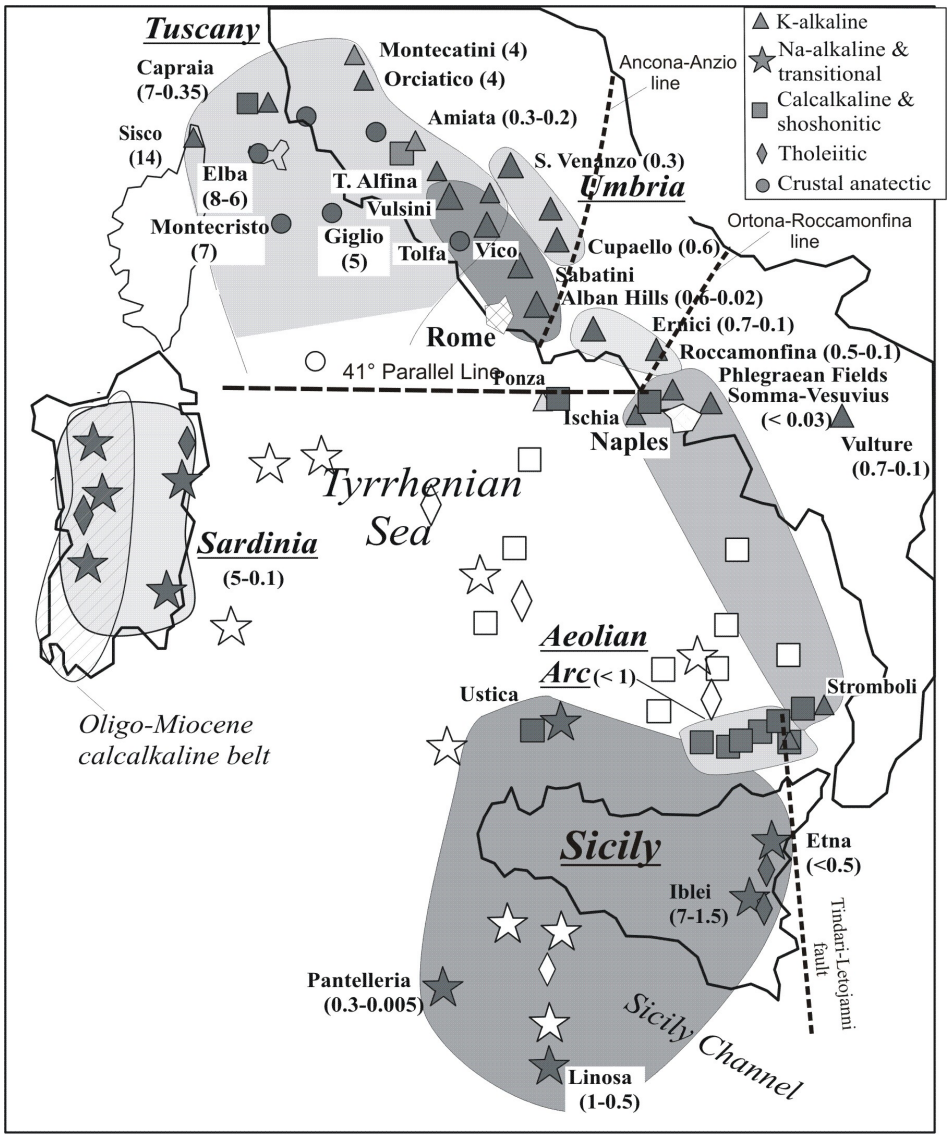

The largest Volcanic risk in the world

VESUVIUS

Cartoon showing the three-dimensional geodynamic scheme of the Tyrrhenian basin and bordering volcanic areas, including the subduction of the Ionian-Adria lithosphere in

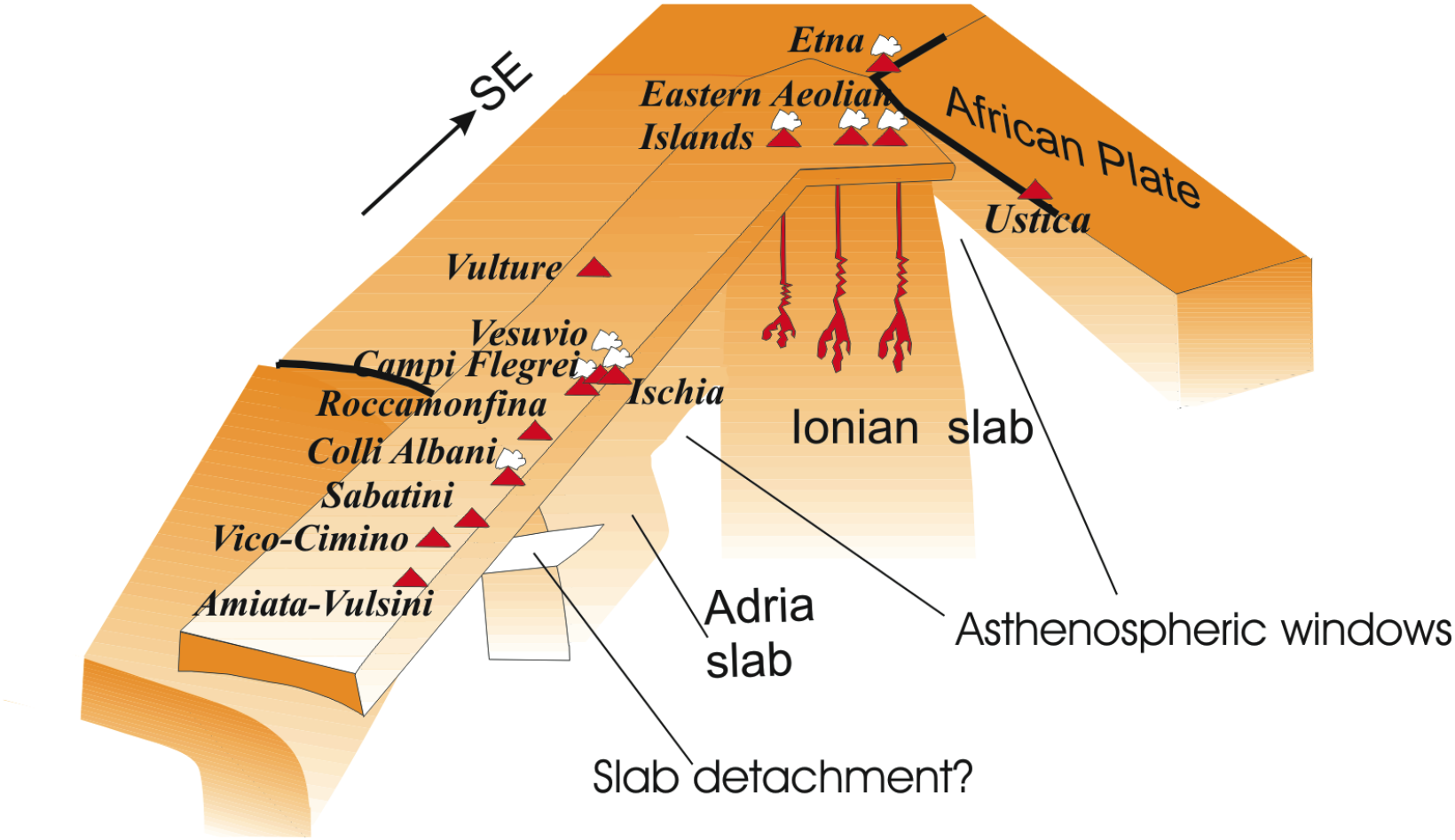

Mt. Vesuvius cone

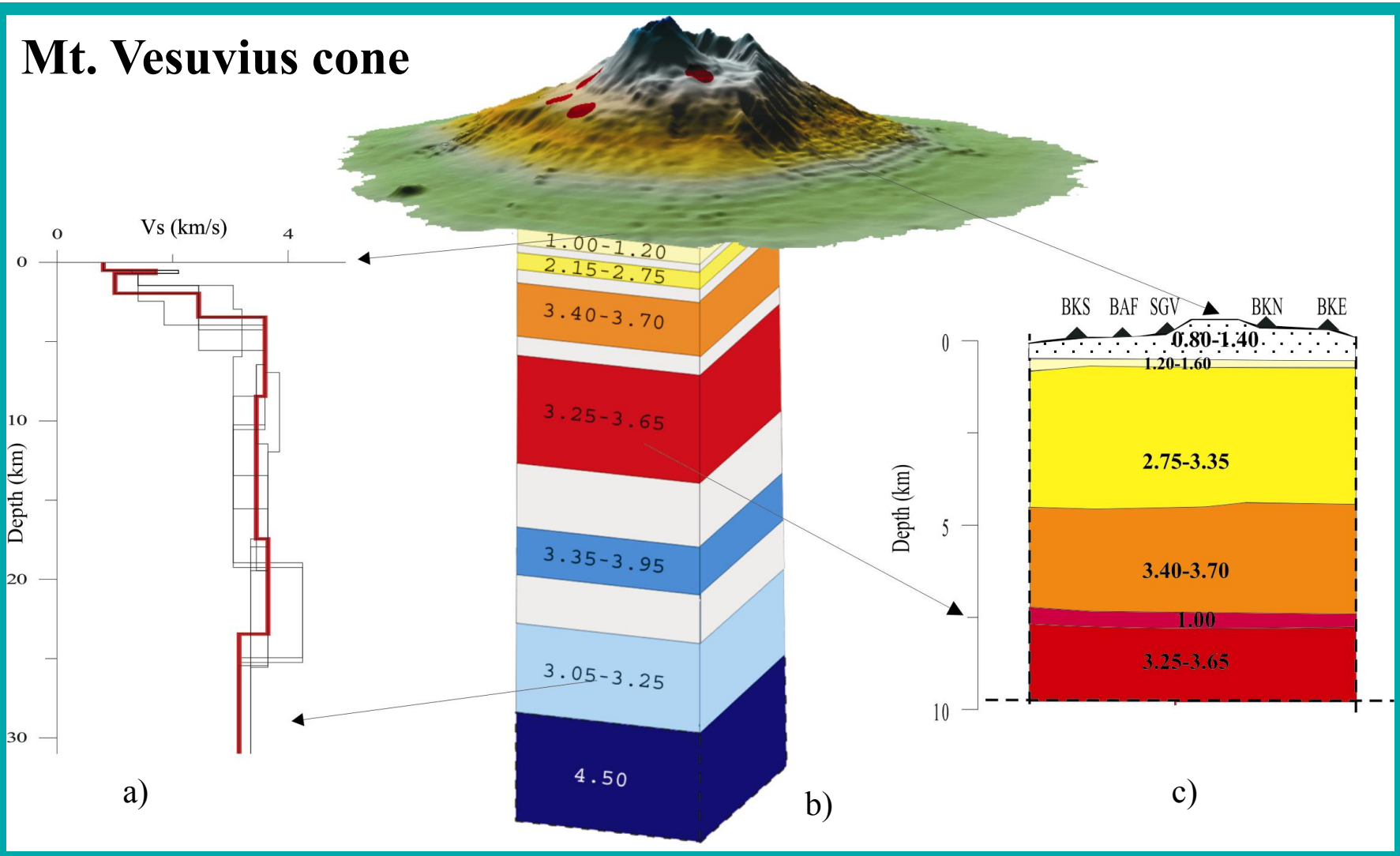

(a) Hedgehog solutions (lines) from the average Rayleigh wave group velocity dispersion curve computed, in the period range 0.3-2 s, for all stations on **Mt. Vesuvius cone** (BAF, BKN, BKS, BKE, SGV), and regional group (T=10-35s) and phase (25-100s) velocities.
(b) The chosen Vs models are shown along SE-NW-SW-NE cross-sections through Somma-Vesuvius. The grey bands indicate the boundaries between layers, that can well be transition zones in their own right, and the group of numbers indicate the ranges for V_S in km/s.
(c) Uppermost part of the chosen model, if we impose, as a priori information, the value of 1.0km/s (Auger et al., 2003), for the low velocity layer at 8km of depths (this ultralow-velocity layer is present in all solutions).

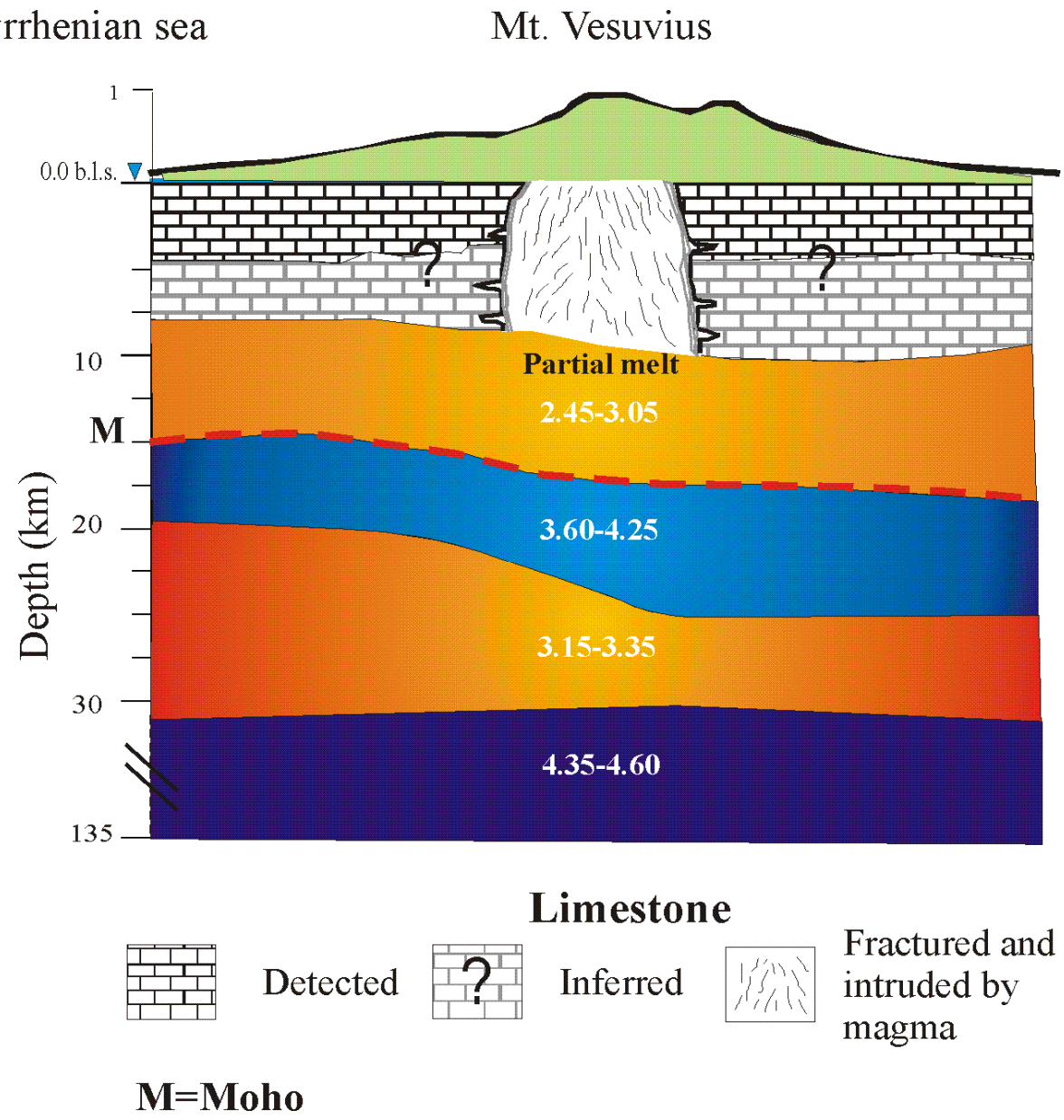

Schematic model of the crust and uppermost mantle at Mt. Vesuvius. The possible ranges of Vs are given in the figure while the uncertainty (about 1-2 km) of the thickness for each layer is omitted for clarity reasons. The Moho depth (M) is shown as dashed line.

Comparison between Campi Flegrei and Vesuvian structural models

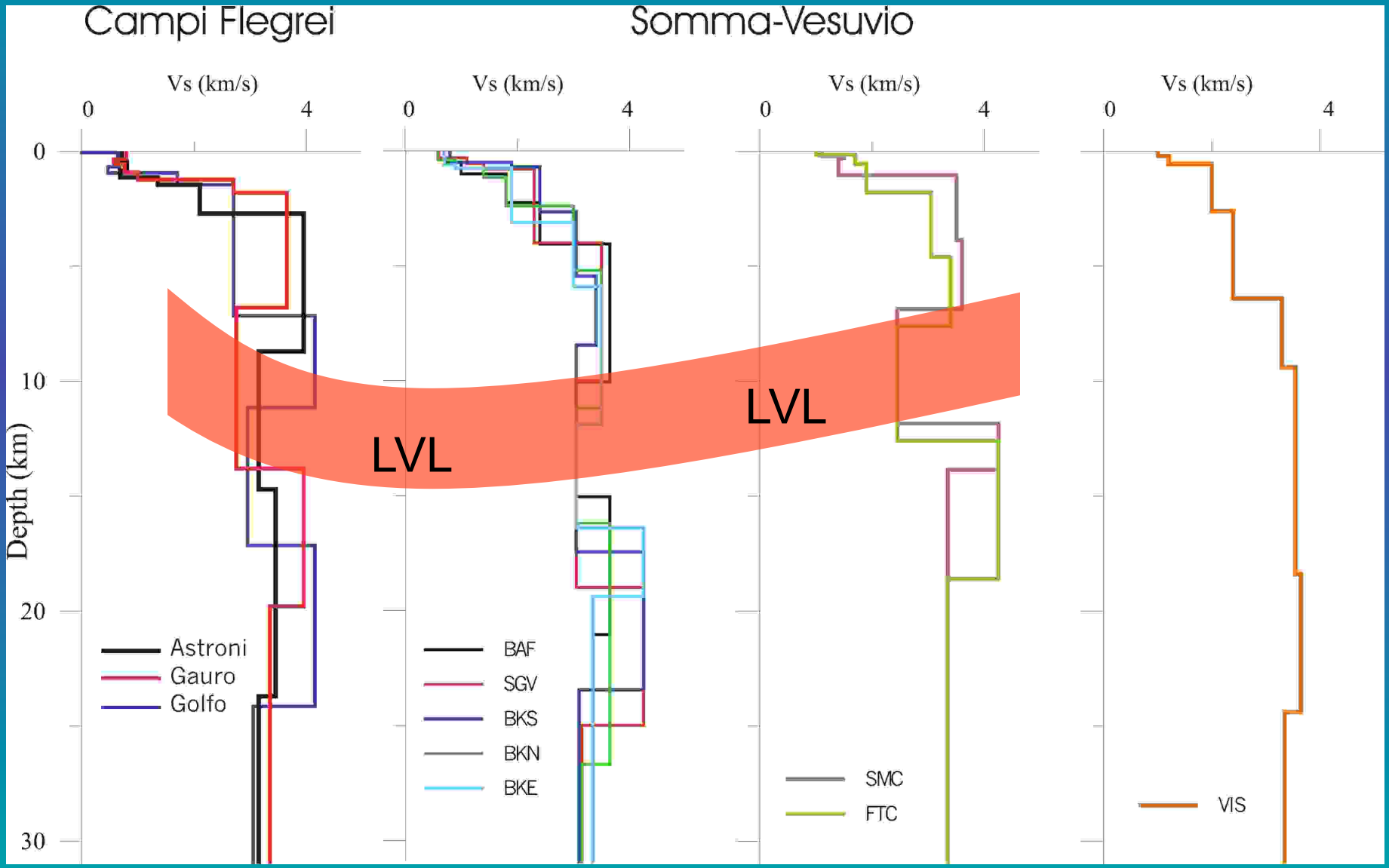

Map of Campi Flegrei and Vesuvio volcanic areas

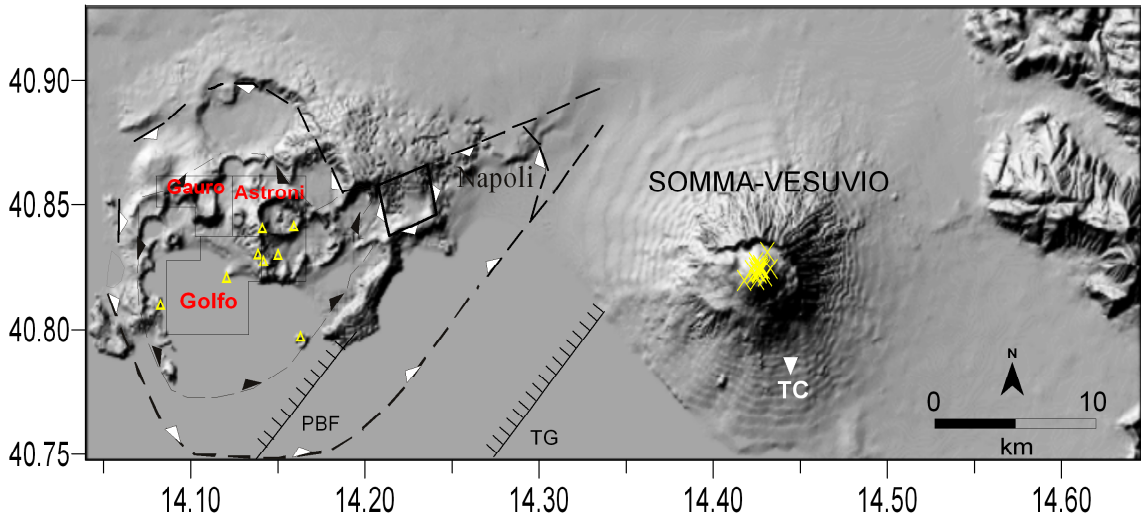

Vs models along a SW-NE cross-section through the Vesuvio-Campi Flegrei paths. The grey bands indicate the boundaries between layers, that can well be transition zones in their own right.

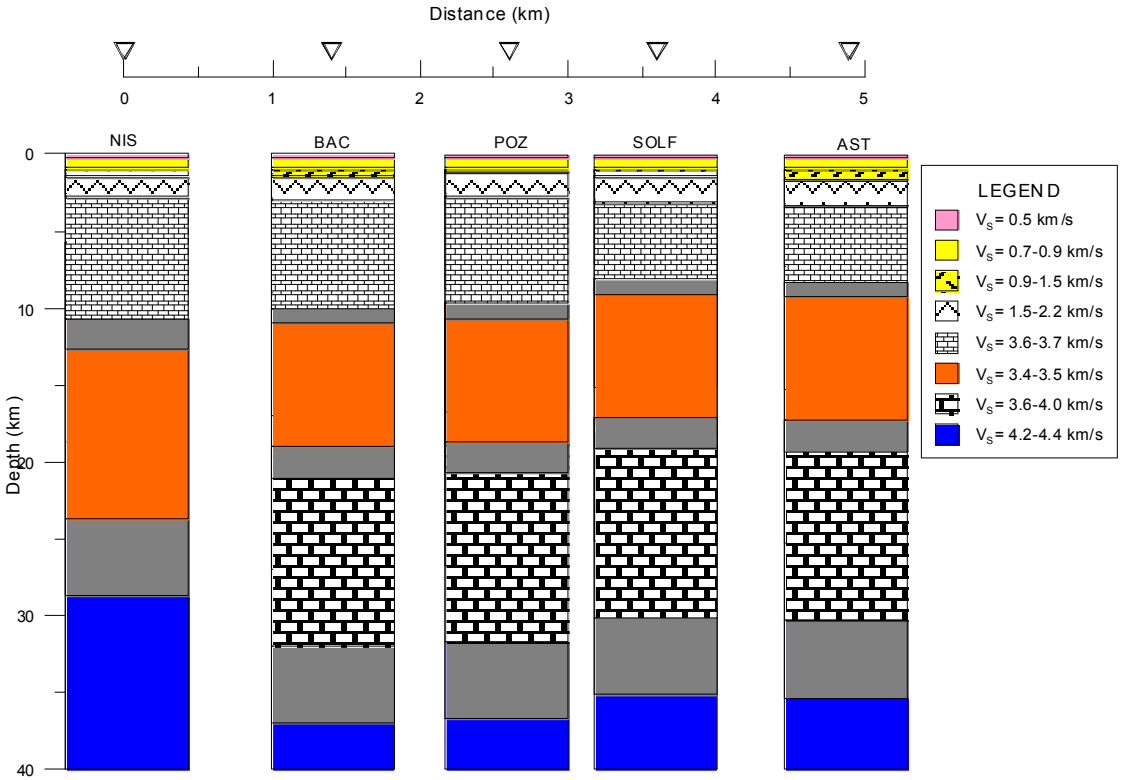

Nunziata, 2009, in press

ETNA

The dynamics of the 2001 eruption as seen by full moment tensor analysis (INPAR method)

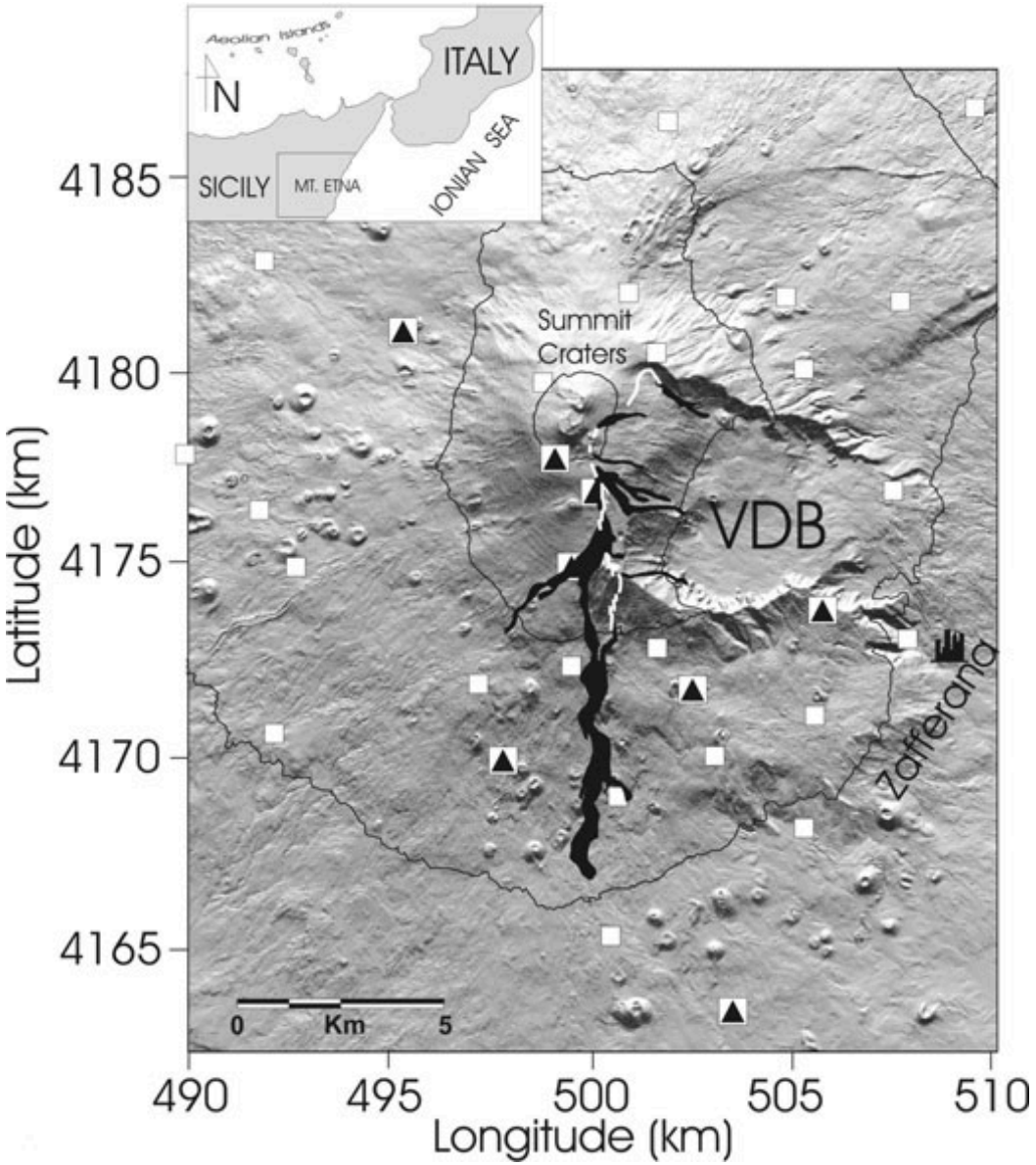

Map of the eruptive scenario of the 2001 eruption: fractures opened between July 12 and 17 (white lines) and lava flows (black stripes) are drawn. VDB indicates the Valle del Bove Caldera.

Seismic stations (white squares: 1-component stations; black triangles: 3-component stations) located in the central part of the volcano and managed by the permanent INGV-CT network (Patané *et al*. 2003).

Moment Tensor Decomposition

The equivalent forces of a seismic point source can be determined by the analysis of the eigenvalues and eigenvectors of the moment tensor.

A common way to decompose the moment tensor is in terms of ISOTROPIC(V), DOUBLE COUPLE (DC) and COMPENSATED VECTOR LINEAR DIPOLE (CLVD) components.

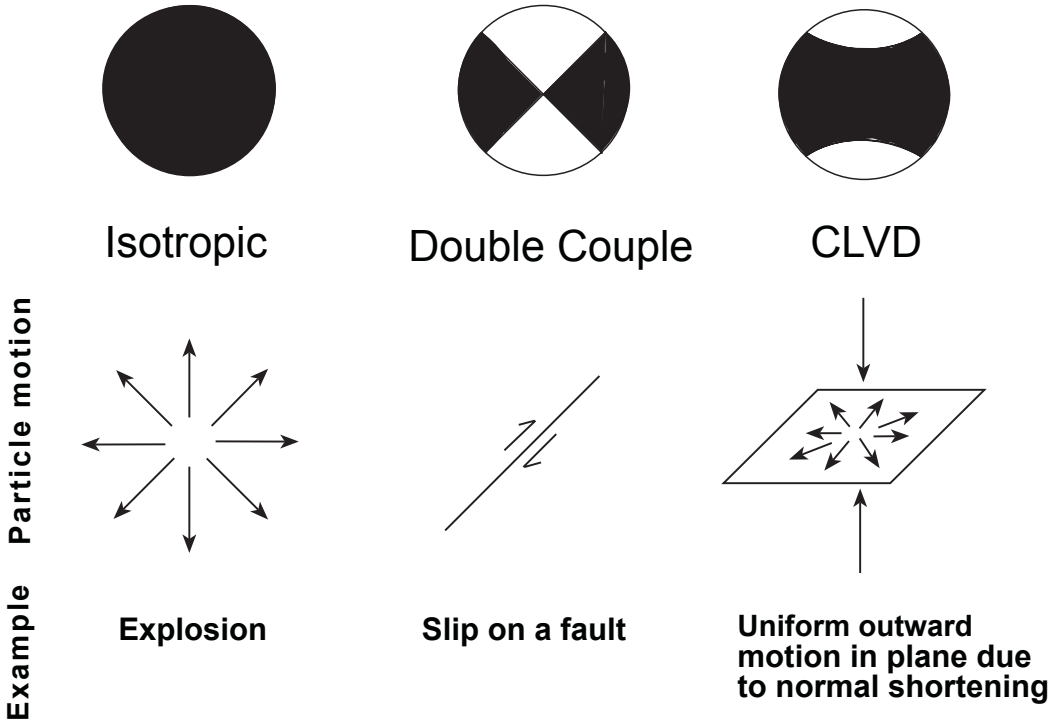

This decomposition is used in INPAR inversion method developed by Sileny and Panza, 1991-1992

(from Frolich & Apperson, 1992)

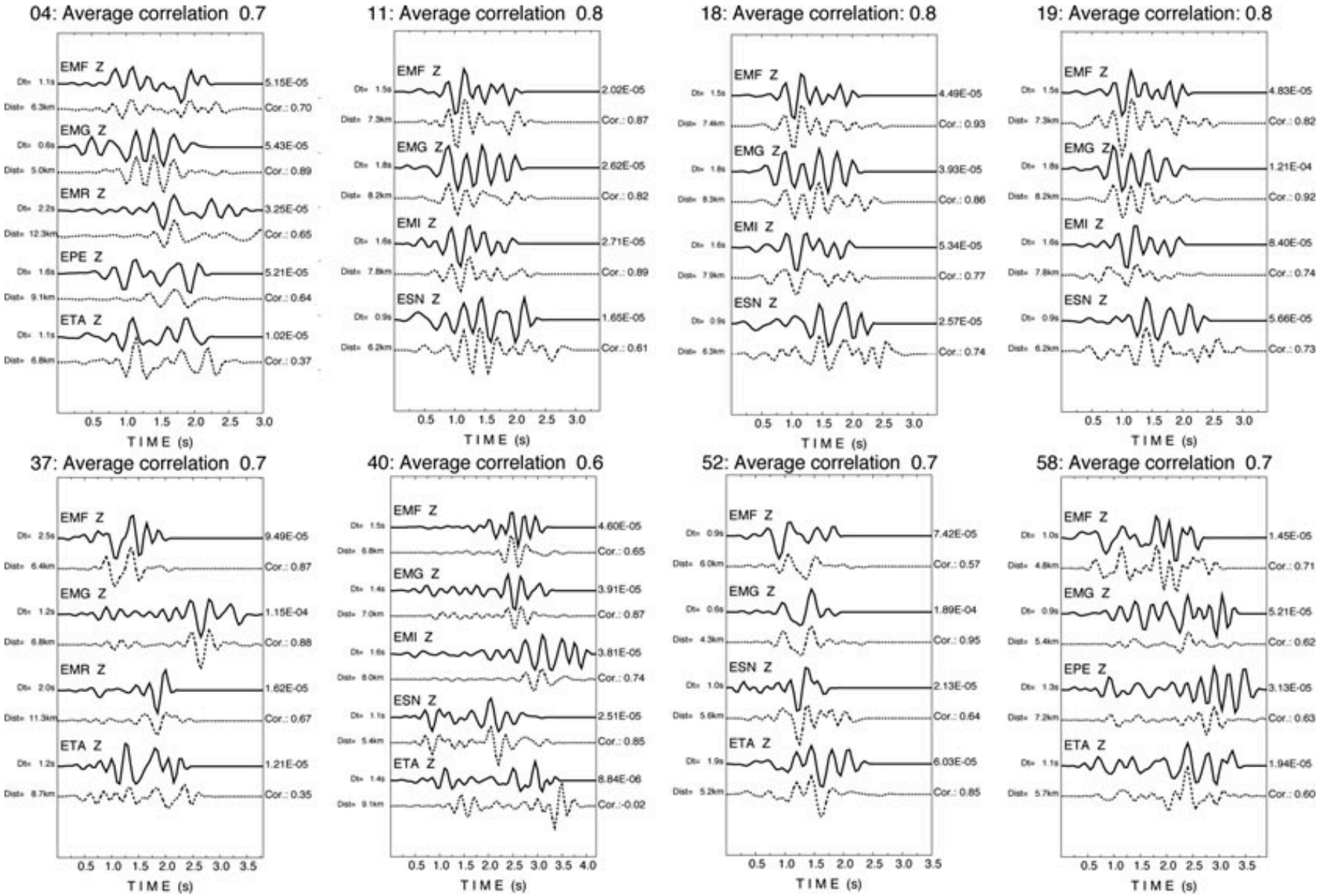

Examples of fit between recorded data (solid line) and synthetics (dotted line). For each signal we report, on the left, the origin of the time window of the signal selected in the inversion and the epicentral distance, whilst the maximum amplitudes and the correlation value (Cor.) are given on the right.

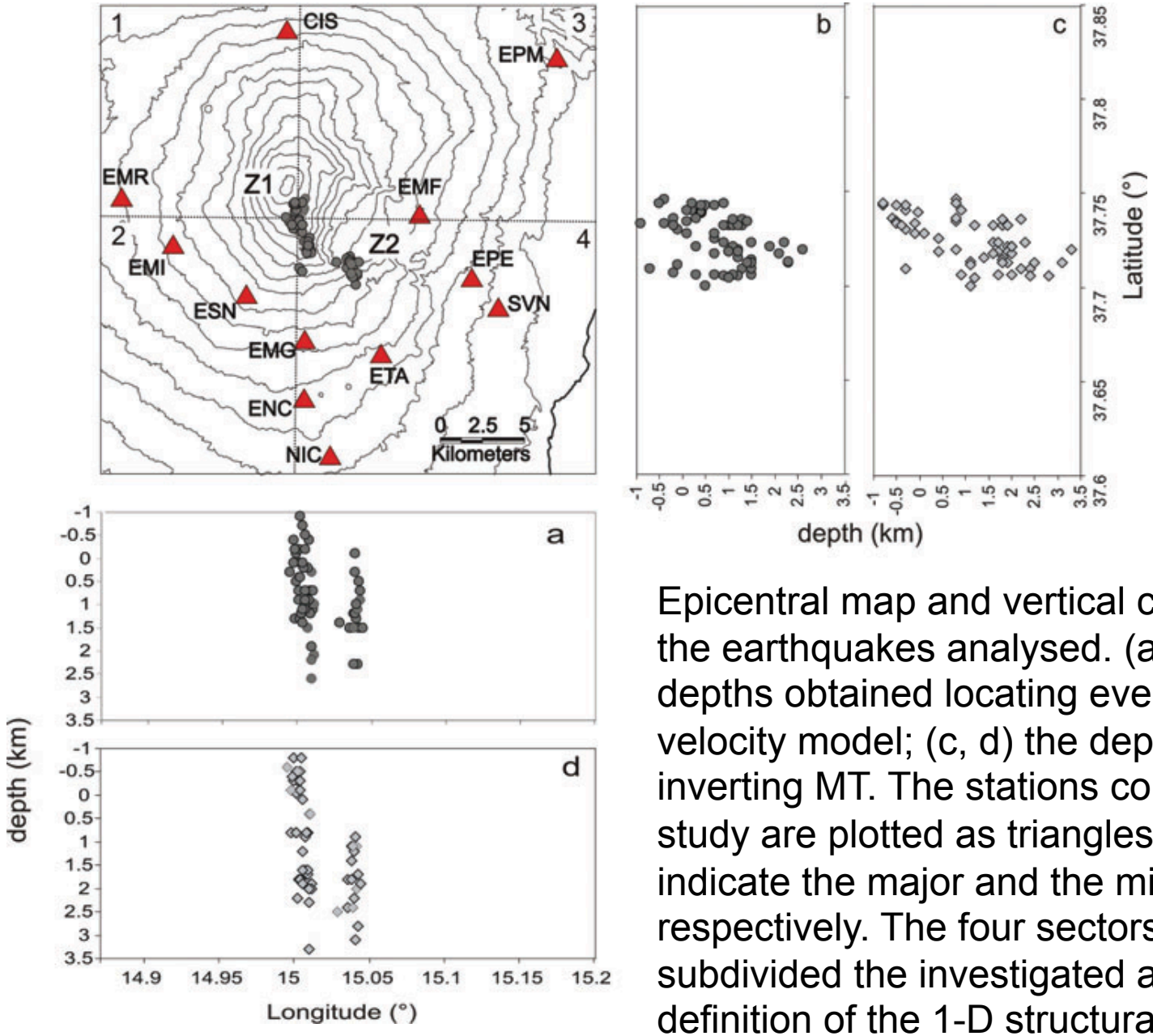

Epicentral map and vertical cross-sections of the earthquakes analysed. (a, b) Hypocentral depths obtained locating events with the 3-D velocity model; (c, d) the depths attained inverting MT. The stations considered in this study are plotted as triangles. Z1 and Z2 indicate the major and the minor cluster, respectively. The four sectors in which we subdivided the investigated area for the definition of the 1-D structural models are traced as well.

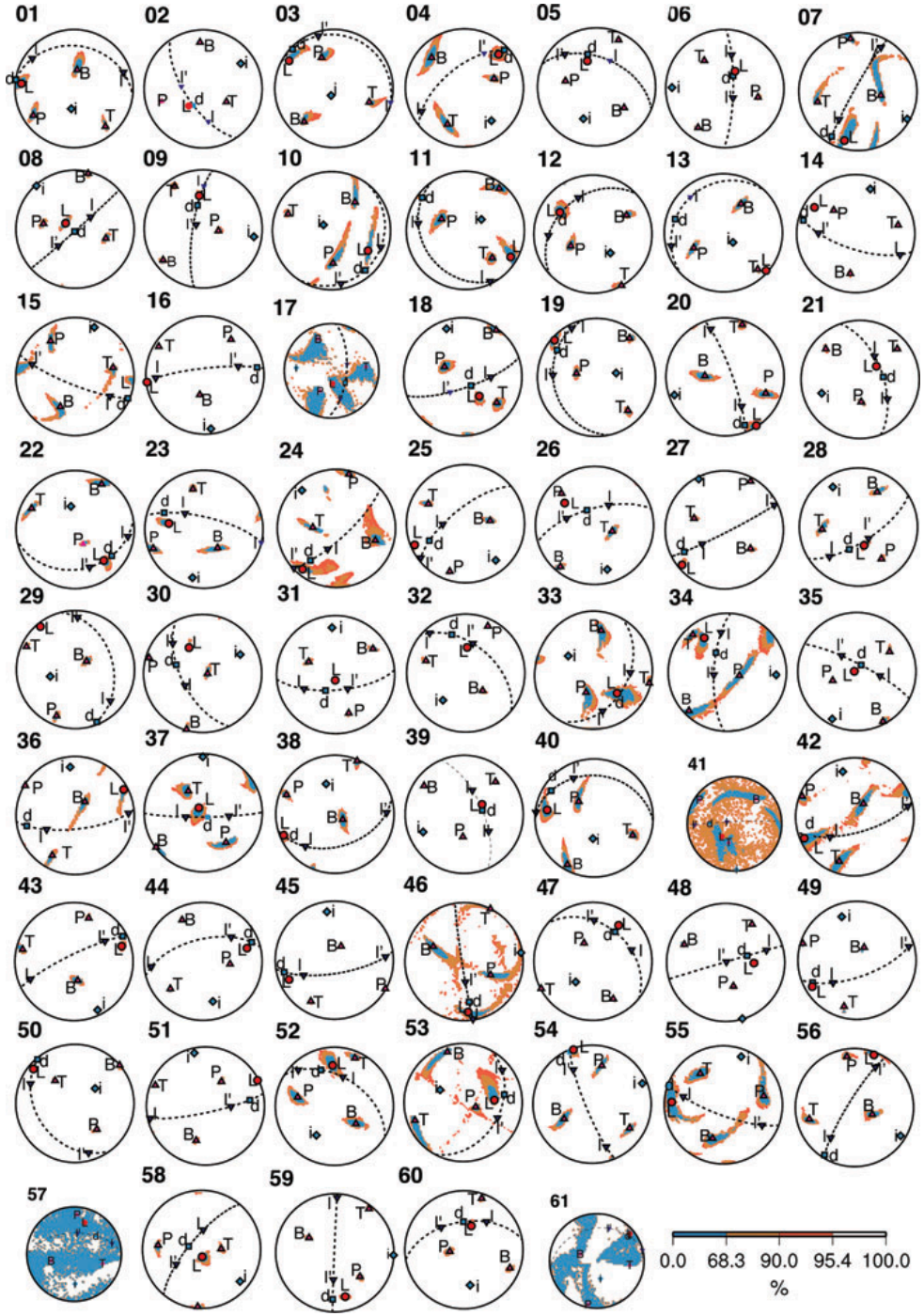

Complete source mechanisms, with confidence error ellipses, represented following Riedesel-Jordan (1989) formalism. **L** is the vector describing the total mechanism, **d** is the DC vector, **l** and **l'** are the CLVD with major dipole along the tensional and the pressure axes, respectively. **i** represents a pure *V*; T, P and B indicate the tensional, compression and null axes, respectively. Triangles pointing downwards are vectors in the lower hemisphere, triangles pointing upwards are vectors on the upper hemisphere. Hatched areas around the L, P, T and B axes are the projections of the confidence areas onto the focal sphere.

The distance of **L** from the vectors **l**, **d**, **l** and **l'** displays the share of *V*, DC and CLVD components, respectively. Events 17, 41, 57 and 61 show very large error areas and are not considered in the discussion.

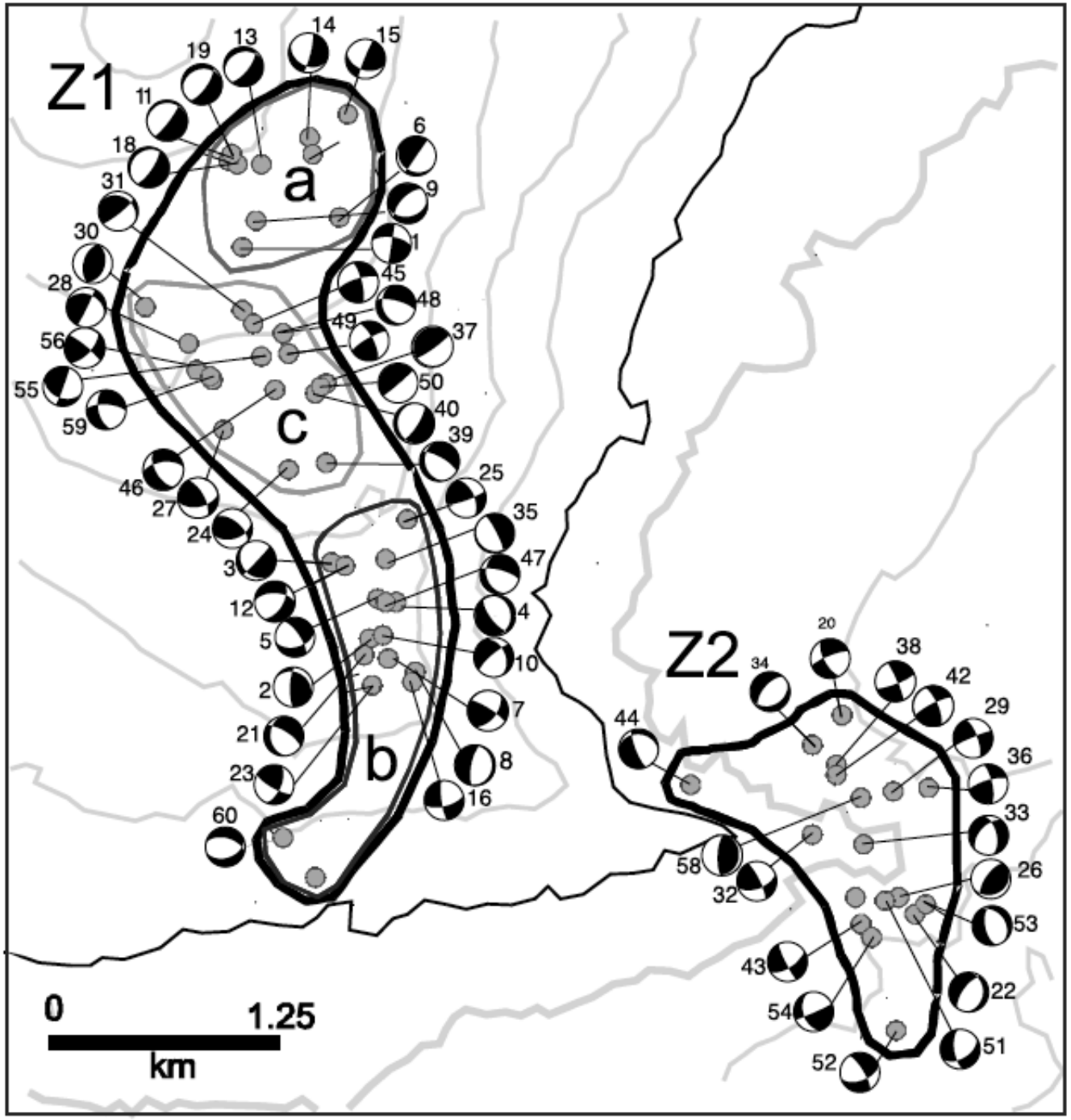

Focal mechanisms (best double-couple) obtained from moment tensor inversion (INPAR).

Z1 (a–c) and Z2 sectors correspond to spatio-temporal grouping of the investigated seismicity.

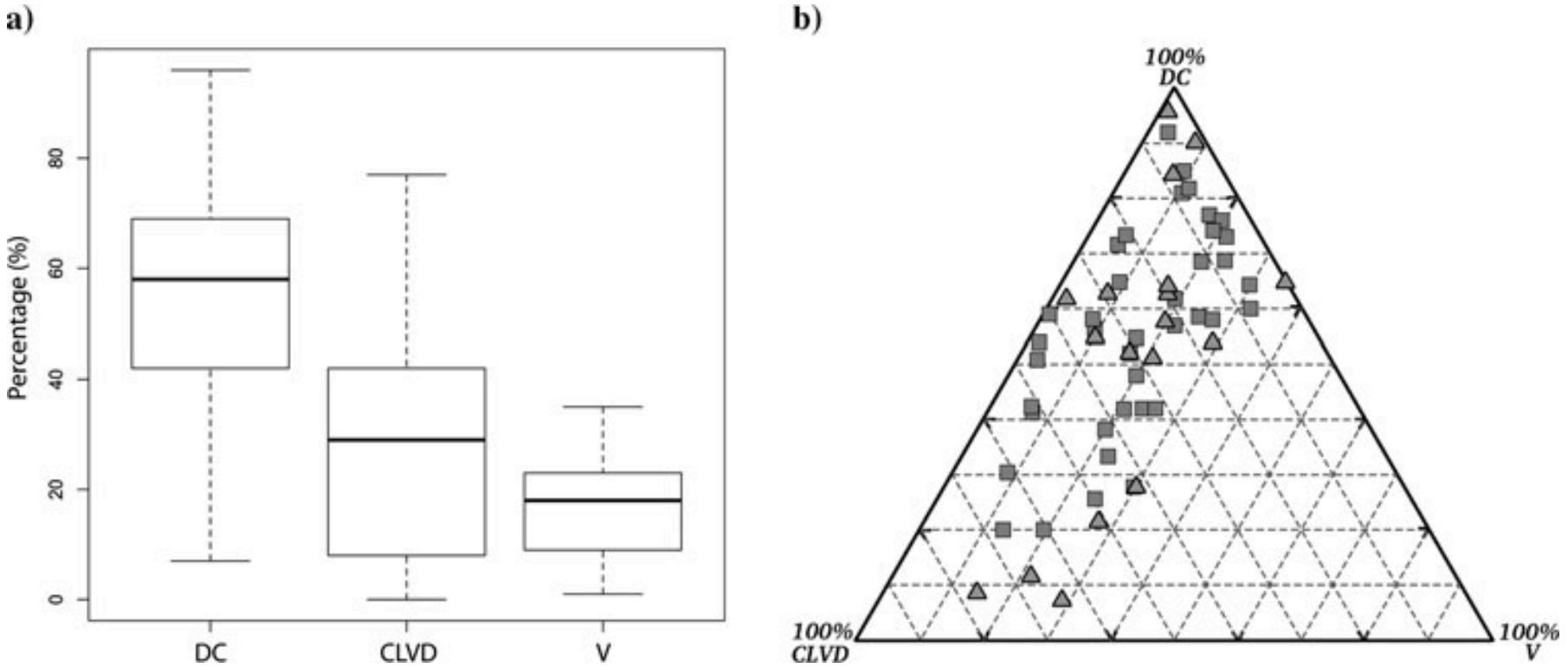

(a) Boxplot for the percentages of moment tensor component, DC, CLVD and *V*. The upper and lower ends of the box are drawn at the quartiles, and the bar through the box is drawn at the median. The whiskers extend from the quartiles to the maximum and minimum data values. The box itself contains the middle 50 per cent of the data. If the median line is not equidistant from the hinges, then data are asymmetrically distributed.

(b) (b) Ternary diagram showing the percentage of DC, CLVD and *V* retrieved for the earthquakes located in Z1 (squares) and Z2 (triangles).

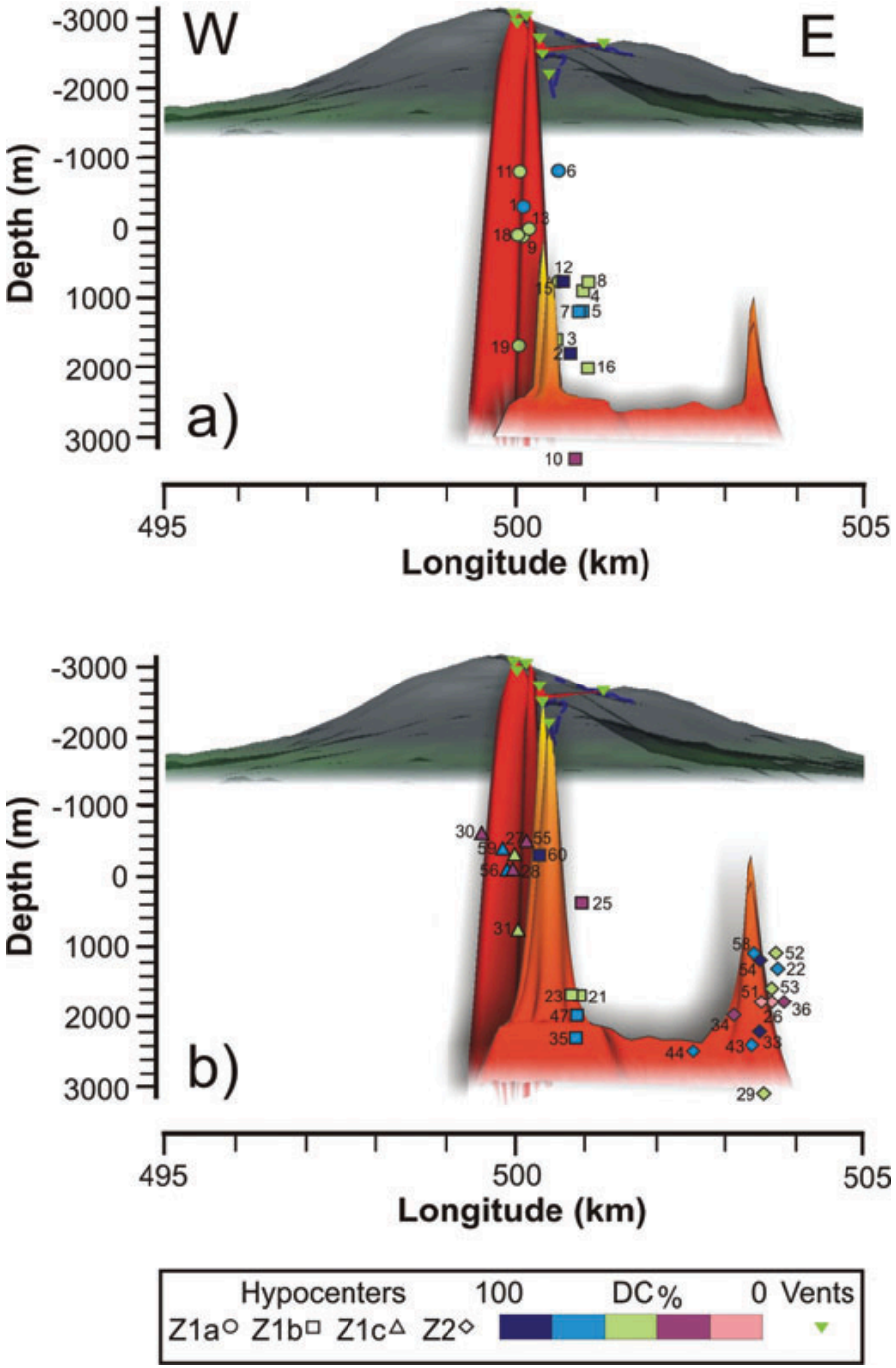

Speculative model of the central feeding system (red) and evolution of eccentric dykes (orange and yellow) during the analysed period (2001 July 12–18).

Intrusions from the central feeding system (a) precede the rise of eccentric dykes (b). Seismicity is plotted with different symbols for each of the identified zones with colours that represent the DC component percentages. The numbers are associated with earthquakes listed in Table 1; events located beyond eccentric dykes are not shown. The fracture system (blue lines) and eruptive vents are also reported.

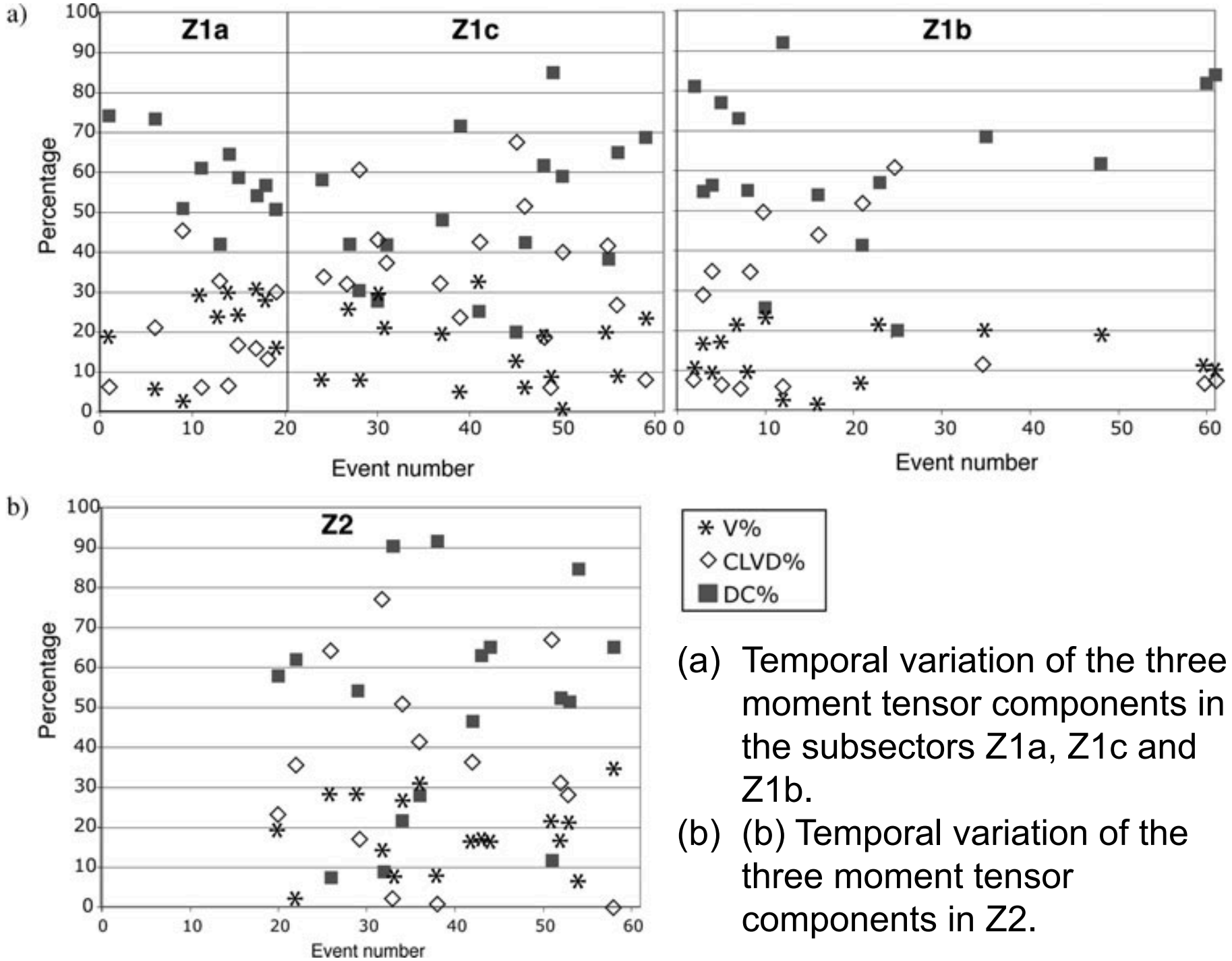

(a) Temporal variation of the three moment tensor components in the subsectors Z1a, Z1c and Z1b.

(b) (b) Temporal variation of the three moment tensor components in Z2.

The source moment tensors retrieved show different focal mechanisms with a predominance of normal faulting (44 per cent) and a few strike slip (30 per cent) and thrust mechanisms (9 per cent), all of them compatible with the complex local stress regime generated by vertical dyke propagation.

The focal mechanisms determined from polarities and INPAR are comparable, within the error areas, for the events with relatively small *V* components (less than 25 per cent) and simple STF.

The northern part of the 2001 eruptive phenomenon is seismically active only for a few hours during the first stage of the swarm (Z1a) with a high percentage of DC components (greater than 70 per cent). At the same time, the deeper portion of Z1b is affected by earthquakes (located 1.0–2.5 km b.s.l.) with significant percentage of CLVD components (20–50 per cent). After 4 hr, the seismic activity stops in Z1a and starts in Z1c, where earthquakes with a significant CLVD component (30–60 per cent) occur as well.

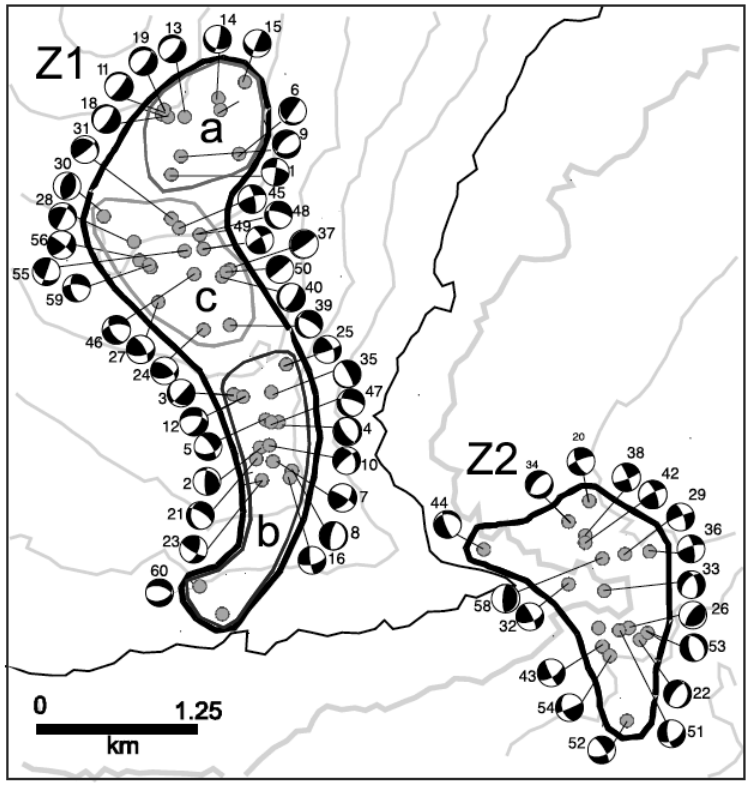

The DC variation observed in the early hours in both sectors Z1ac and Z1b are statistically significant at 95 and 90 per cent confidence levels, respectively.

After the opening of the first fissures system, the intrusive process is facilitated. Then the percentage of non-DC earthquakes increases until, proceeding towards the onset of the eruption, the stress regime imposed by the dyke emplacement dominates again and DC events occur mostly as brittle response of the confining medium. The intrusion of the primitive batch of magma starts in Z1b, at a depth of 2–3 km, aligned along the early surface fractures. The fracture system develops towards N and intersects, on July 17, the highly fractured zone (Z1a) where old batches of magma were residing.

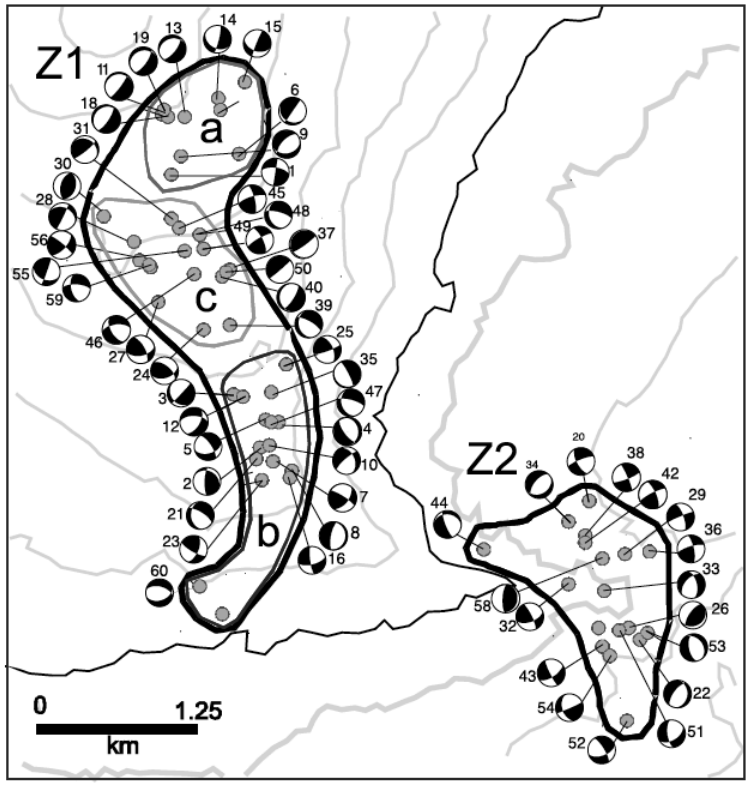

The intrusion started in Z1b, reaches the surface on July 18 and outpours gas-rich magma with primitive composition and basement xenoliths, testifying to a high-velocity uprising dyke.

The sequence in Z2 area starts later, on July 13, and the maximum depth of hypocenters is comparable to that of Z1. A still immature process of magma reclimbing can explain the erratic variation of observed DC percentage, not statistically significant at 95 per cent confidence level. These features, together with the trend of the focal depths, suggest a magma intrusion parallel to that occurring under Z1b that is tentatively associated with the same magma reservoir, which fed the lowermost part of the 2001 fracture system.

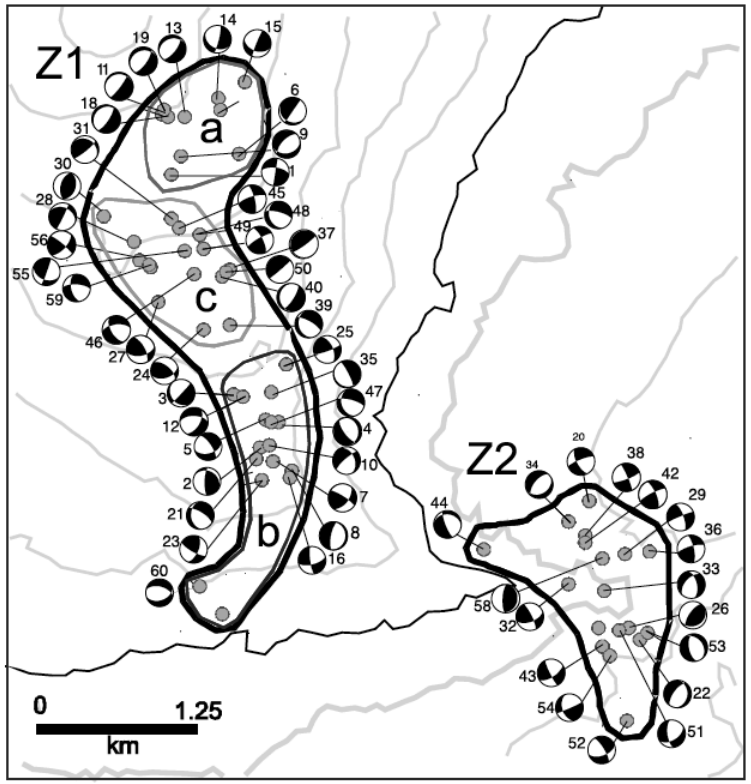

The intrusion stops at around the sea level, where it loses the necessary pressure to overcome the lithostatic load.

CONCLUSIONS

1 - At the beginning of the seismic swarm, the dominant component of the seismic source tensor is double-couple (around 65% on average and statistically significant at 95% confidence level).
2 - In the following hours the non-double-couple components increase at the expenses of the double-couple.
3 - Initial dominance of DC correlates well with the system of fractures formed just before the eruption, whereas the subsequent increase of non-double-couple components is explained as the response of the confining rocks to the rising magma and degassing processes.
4 - The type of focal mechanisms retrieved are of normal fault type (44%), strike slip (30%) and thrust mechanisms (9%), and outline a scenario that concurs with the stress regime induced by a dyke injection.
5 - The space–time analysis of seismic source locations and source moment tensors (1) confirms the evidence of a vertical dyke emplacement that fed the 2001 lateral eruption and (2) adds new insights to support the hypothesis of the injection of a second aborted dyke, 2 km SE from the fractures zone.

CO_2 from upper mantle degassing

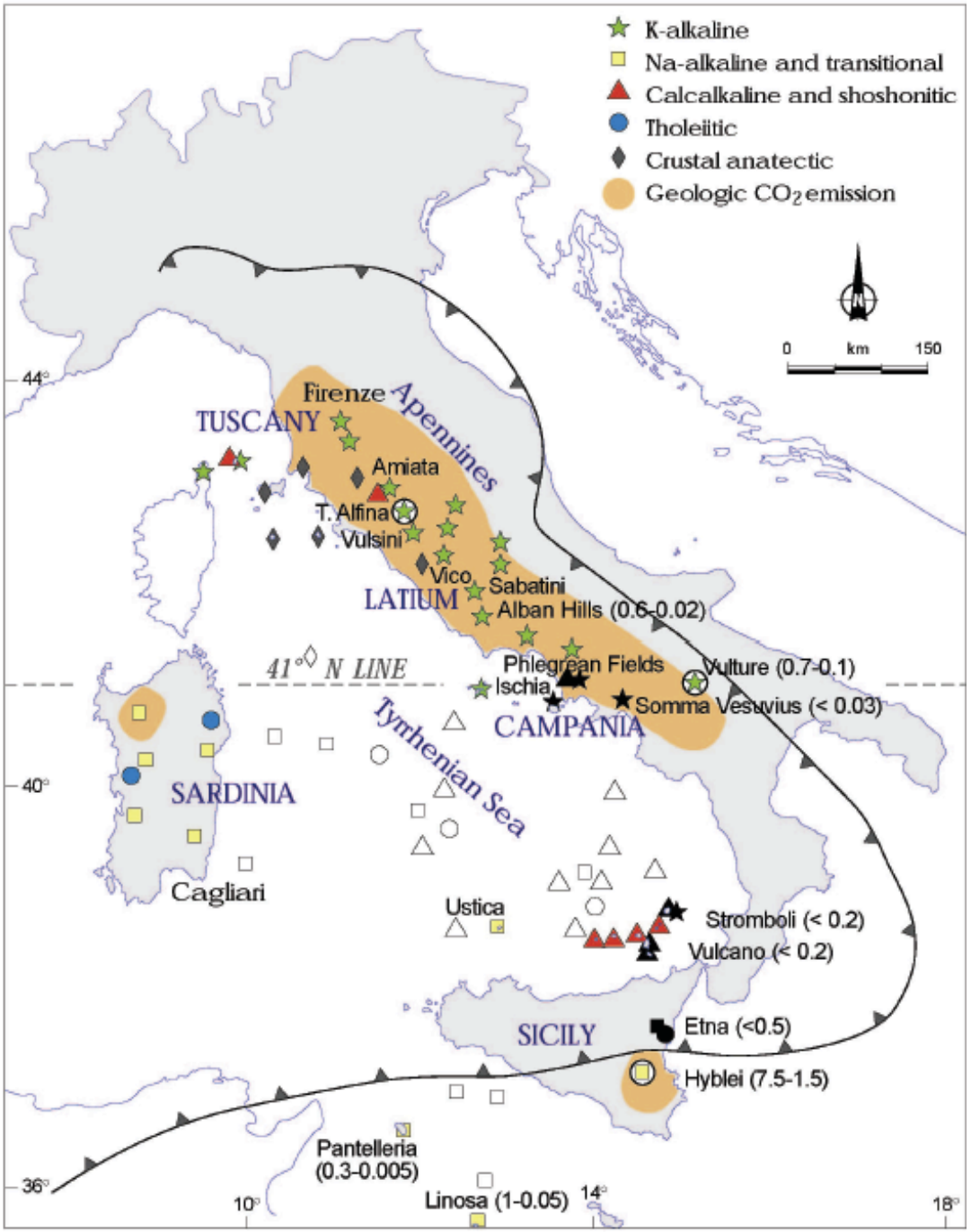

Distribution of main geological CO_2 emission in Italy (orange area), as derived from the online catalogue of Italian gas emissions,(http://googas.ov.ingv.it), and of petrochemical affinities and ages of the main Plio-Quaternary magmatic centers in Italy. Active volcanoes are marked in black. Ages in parenthesis.

(modified from Peccerillo, 2005)

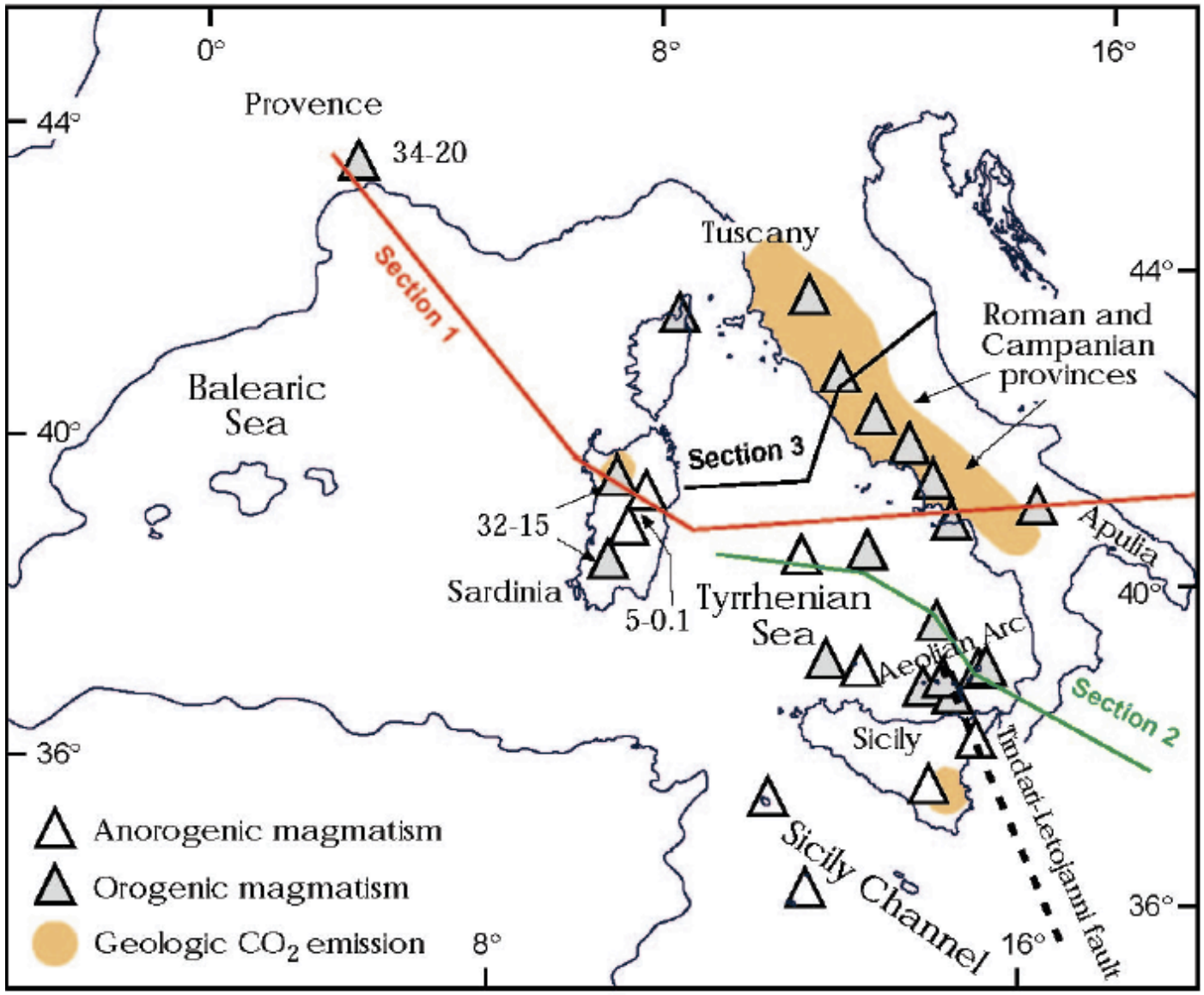

Location of the orogenic and anorogenic Plio-Quaternary volcanism in the Western Mediterranean (from Peccerillo, 2003), with respect to geological CO_2 emission areas.

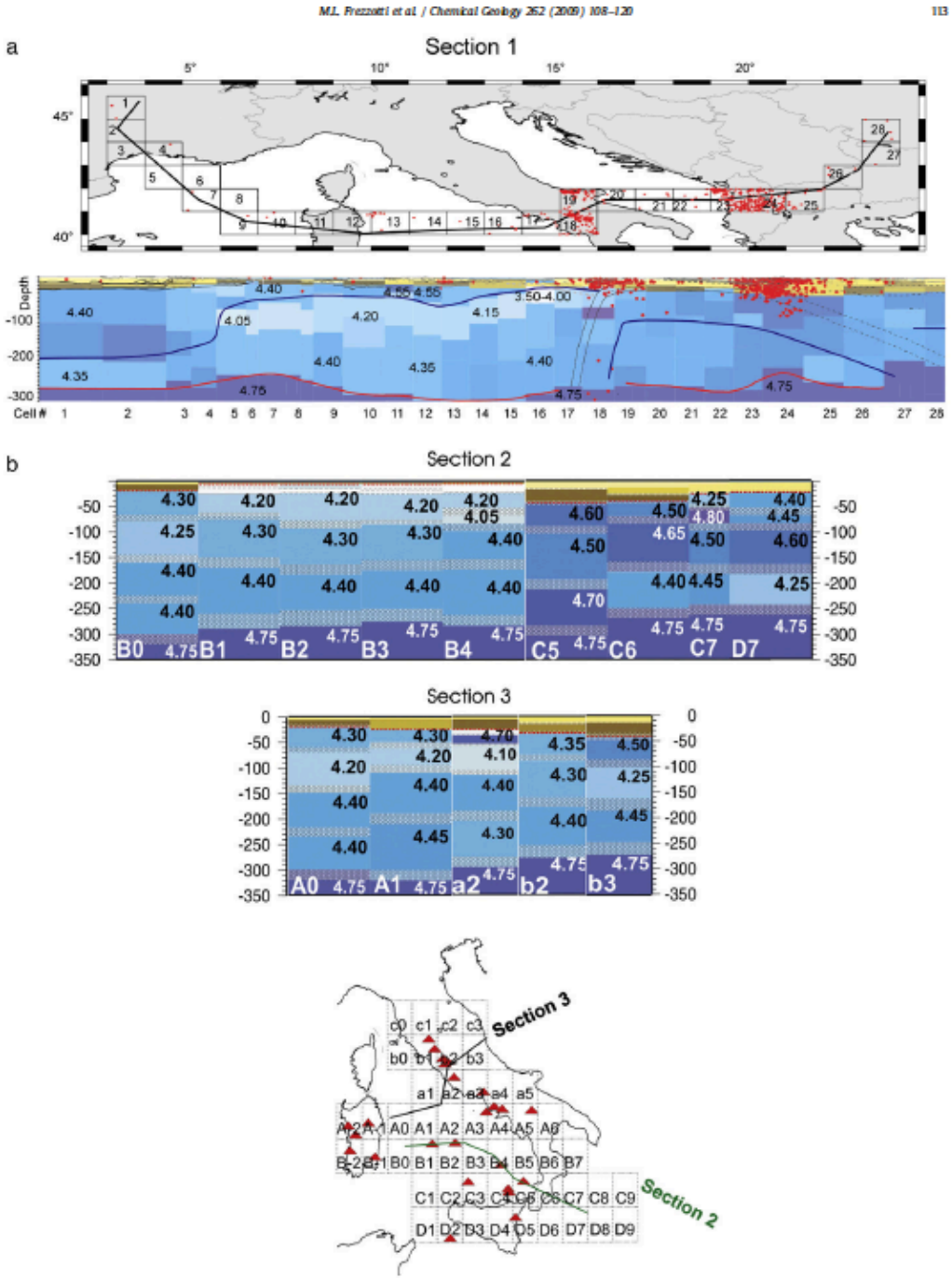

Vs models of the lithosphere-asthenosphere system along representative sections in the Western Mediterranean, built from the cellular Vs model of the Tyrrhenian Sea and surroundings given by Panza et al. (2007b). The hatched zone stands for the thickness variability, while, to avoid crowding of numbers, only the average shear velocity is reported. Vs ranges are given in Panza et al. (2007a). Red triangles indicate recent and active volcanoes.

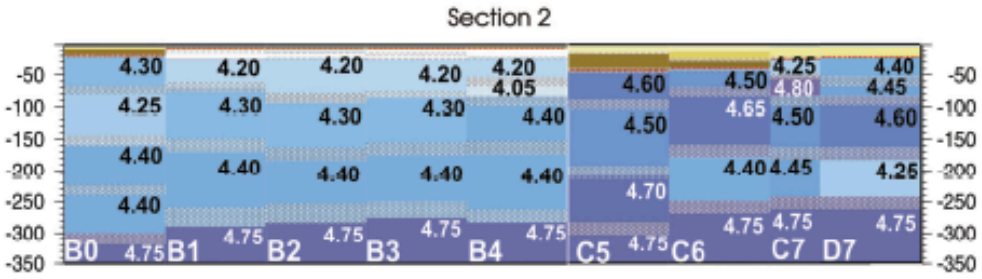

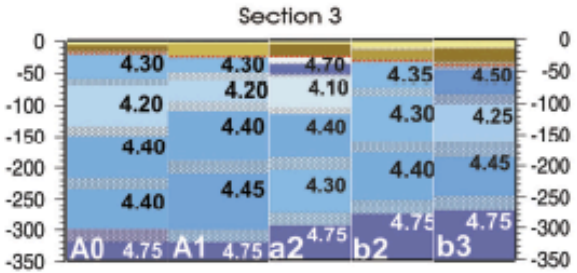

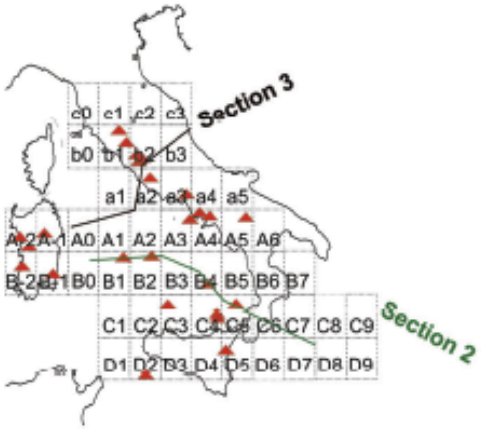

Vs models of the lithosphere-asthenosphere system along other representative sections in the Western Mediterranean, built from the cellular Vs model of the Tyrrhenian Sea and surroundings given by Panza et al. (2007b). In each labeled cell, the hatched zone stands for the thickness variability, while, to avoid crowding of numbers, only the average shear velocity is reported. The Vs ranges of variability are given in Panza et al. (2007a). Red triangles indicate recent and active volcanoes.

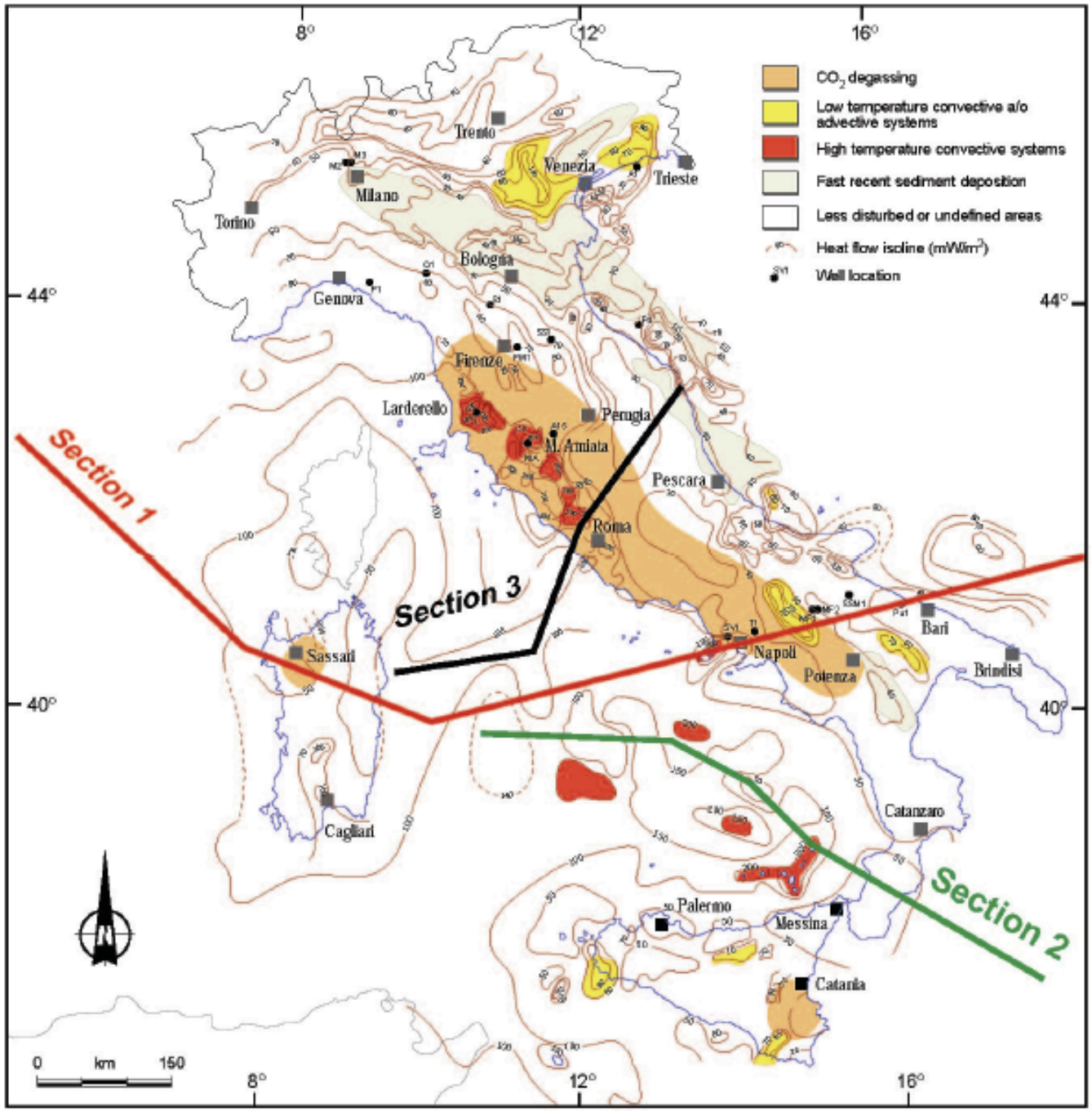

Heat flow map of Italy reporting the location of major CO_2 degassing areas. Most non-volcanic CO_2 emission occurs in areas of normal heat flow. Local high heat flow is associated with subsurface magmas and includes CO_2 fluxes from major geothermal systems (Larderello and Monte Amiata, in Tuscany). Numbered lines represent the pathway of sections just illustrated.

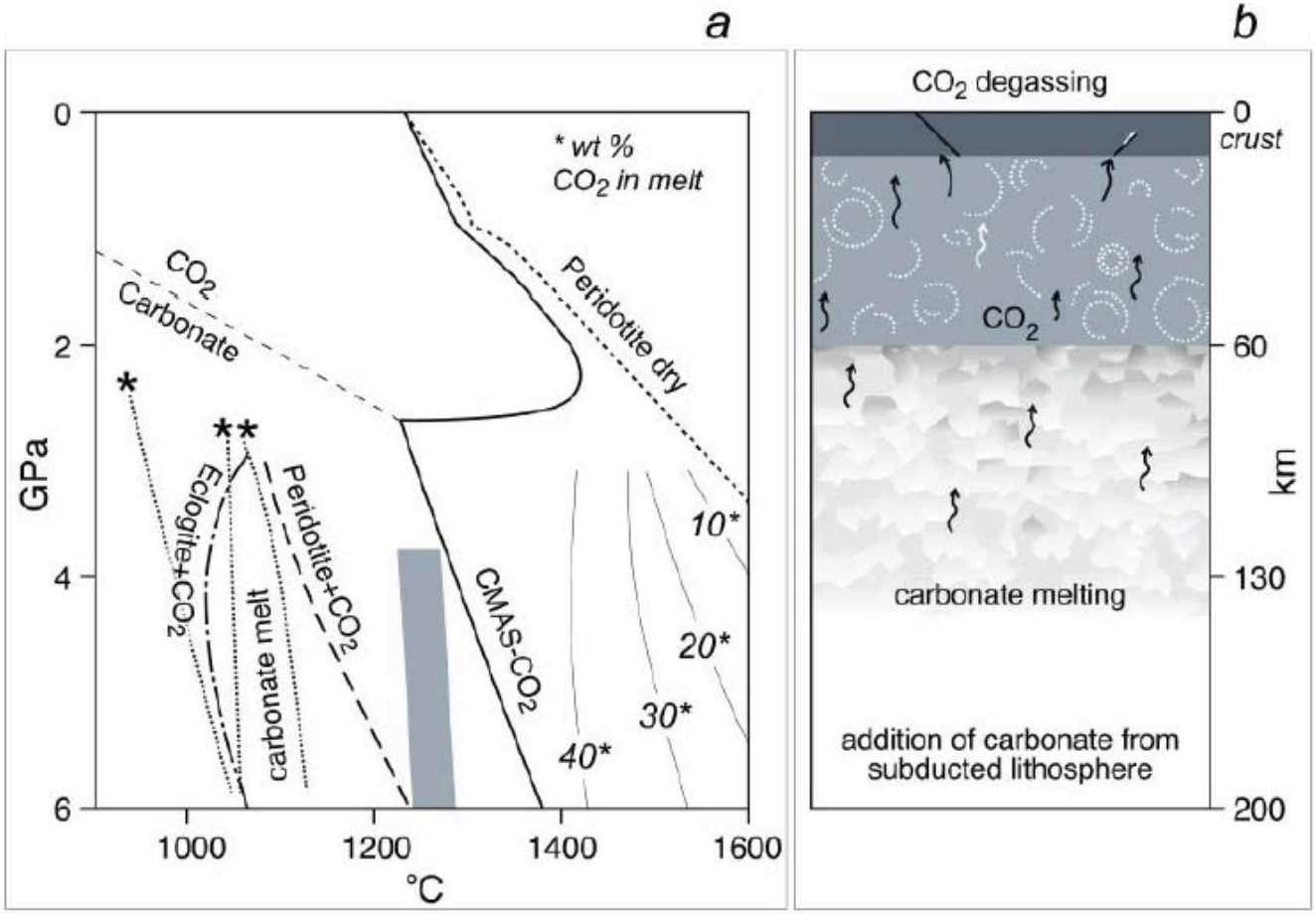

Lithosphere - asthenosphere degassing beneath the Western Mediterranean.
a) Pressure-temperature diagram showing the effects of CO_2 on the *solidus* of carbonated lithologies in the mantle: CMSA - CO_2, and peridotite - CO_2 (2.5 wt %). The effect of carbonates on the composition of melts generated at increasing temperature is reported as wt % CO_2. Gray area = estimated present-day mantle temperatures at the inferred pressures.

b) Present mantle processes and metasomatism beneath the Western Mediterranean. Melting of sediments and/or continental crust of the subducted Adriatic-Ionian (African) lithosphere, generates carbonate-rich (hydrous-silicate) melts at P > 4 GPa (130 km) and T > 1260°C. Due to their low density and viscosity, such melts can migrate upward through the mantle, forming a 70 km thick carbonated partially molten CO_2-rich mantle layer recorded by tomographic images. Upwelling of carbonate-rich melts to depths less than 60 - 70 km, induces massive outgassing of CO_2 in the lithospheric mantle, with cessation of Vs attenuation. Buoyancy forces, probably favored by fluid overpressures, and tectonics might allow further CO_2 upwelling to the Moho and the lower crust, and, ultimately, outgassing at the surface.

Earthquake prediction

and

non-linear dynamics

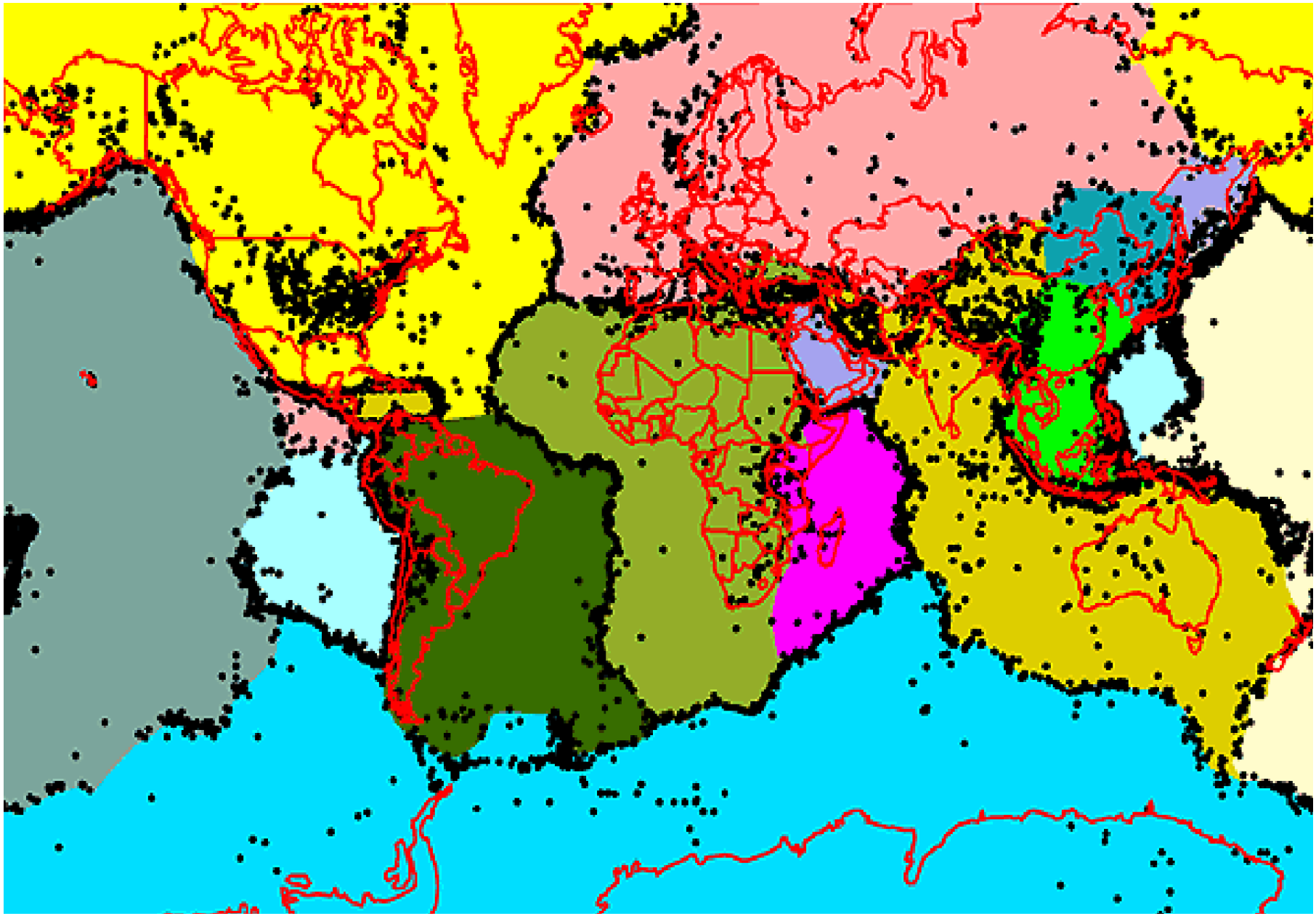

Earthquakes and lithospheric plates

Characteristics of the lithosphere

Scale invariance of earthquake distribution in time and space

Self-organization of earthquake occurence

Non-linear mechanics of earthquake generation

Statistical features of earthquake sequences

Strongly suggest that the lithosphere behaves as a non-linear and possibly deterministic chaotic system (Keilis-Borok, 1990).

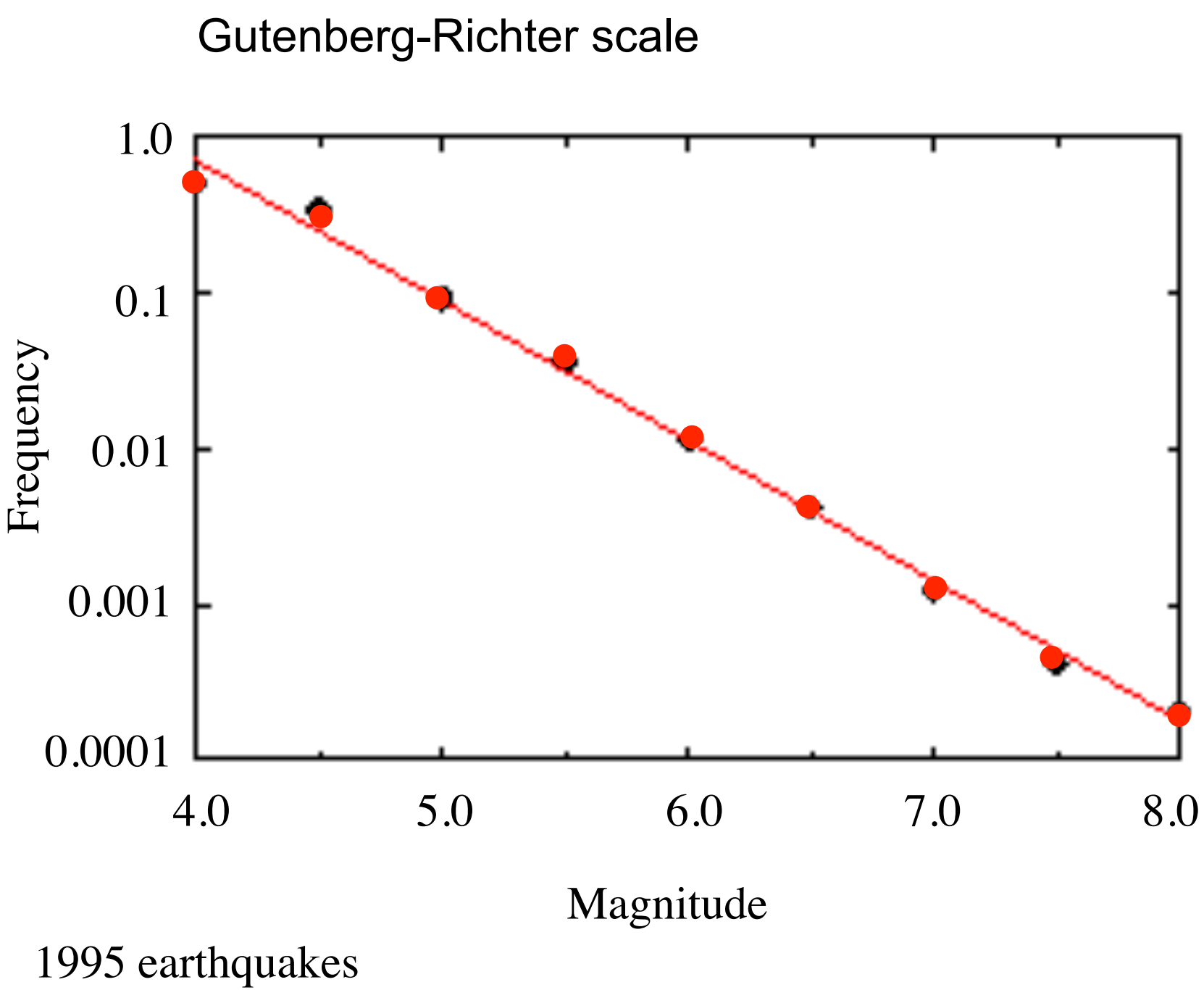
Gutenberg-Richter scale
1.0
0.1
0.01
0.001
0.0001
Frequency
4.0
5.0
6.0
7.0
8.0
Magnitude
1995 earthquakes

The Gutenberg-Richter log-linear law supports that the whole lithosphere is a self-organized system in critical state, i.e., a force is acting contemporaneously over all the plates and distributes the energy over the whole lithospheric shell, a condition that can be well satisfied by a force acting at the astronomical scale (e.g. tidal drag).

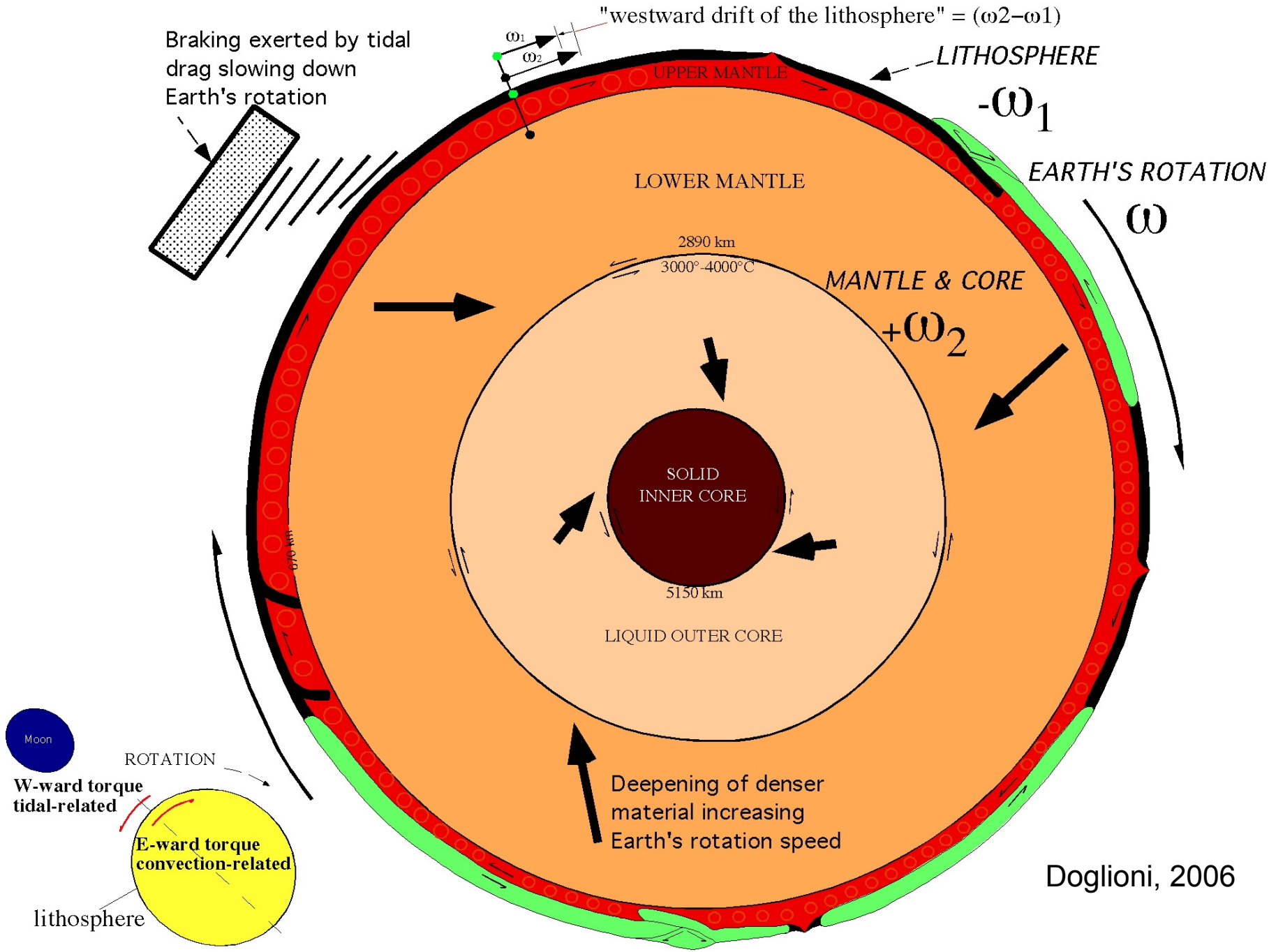
"westward drift of the lithosphere" = (ω2−ω1)
Braking exerted by tidal drag slowing down Earth's rotation
ω1
ω2
LITHOSPHERE
-ω1
UPPER MANTLE
EARTH'S ROTATION
ω
LOWER MANTLE
2890 km
3000°-4000°C
MANTLE & CORE
+ω2
SOLID INNER CORE
5150 km
LIQUID OUTER CORE
Moon
ROTATION
W-ward torque tidal-related
E-ward torque convection-related
lithosphere
Deepening of denser material increasing Earth's rotation speed
Doglioni, 2006

DIALOGO
DI
GALILEO GALILEI LINCEO
MATEMATICO PRIMARIO
DELLO STVDIO DI PISA.
E Filosofo, e Matematico primario del
SERENISSIMO
GR. DVCA DI TOSCANA.
MASSIMI SISTEMI DEL MONDO
TOLEMAICO, E COPERNICANO.

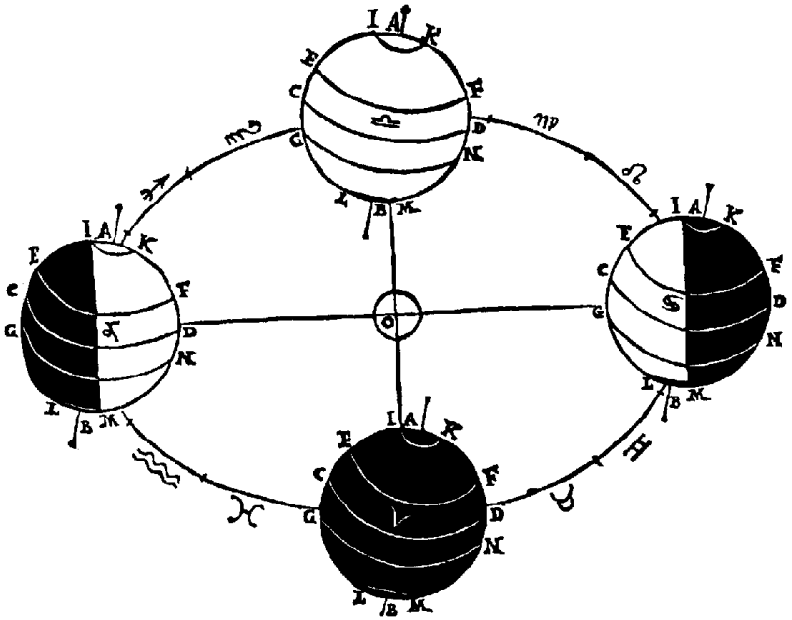

Earth tides are used by Galileo to prove the double motion of the Earth.

DIALOGO, IV giornata

The Gutenberg-Richter law

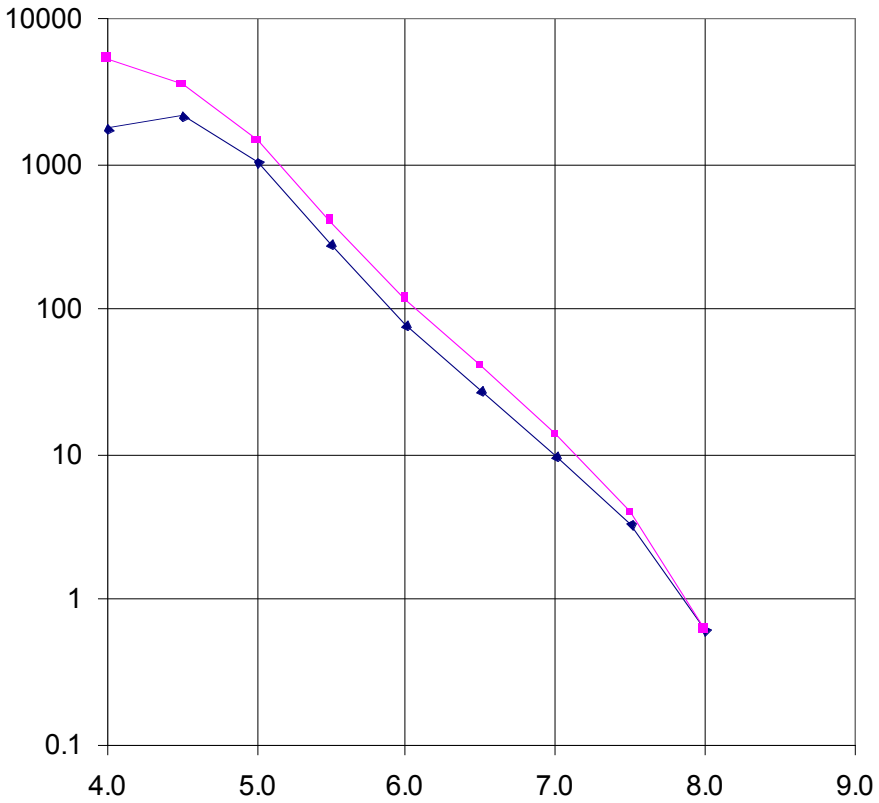

Averaged over a large territory and time the number of earthquakes equal or above certain magnitude, N(M) scales as:

$$\log_{10}N(M) = a - bM$$

This general law of similarity establishes the scaling of earthquake sizes in a given space time volume but gives no explanation to the question how the number, N, changes when you zoom the analysis to a smaller size part of this volume.

The Gutenberg Richter law when applied to small (about 200 km in length) regions is linear only over a small magnitude interval [3-4.5].

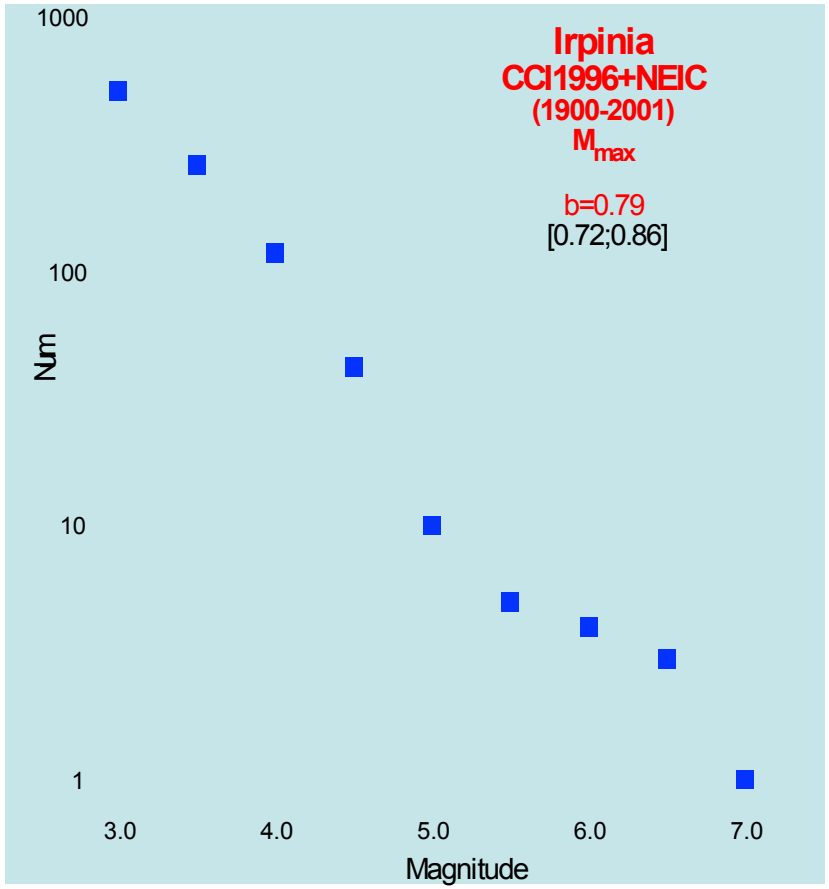

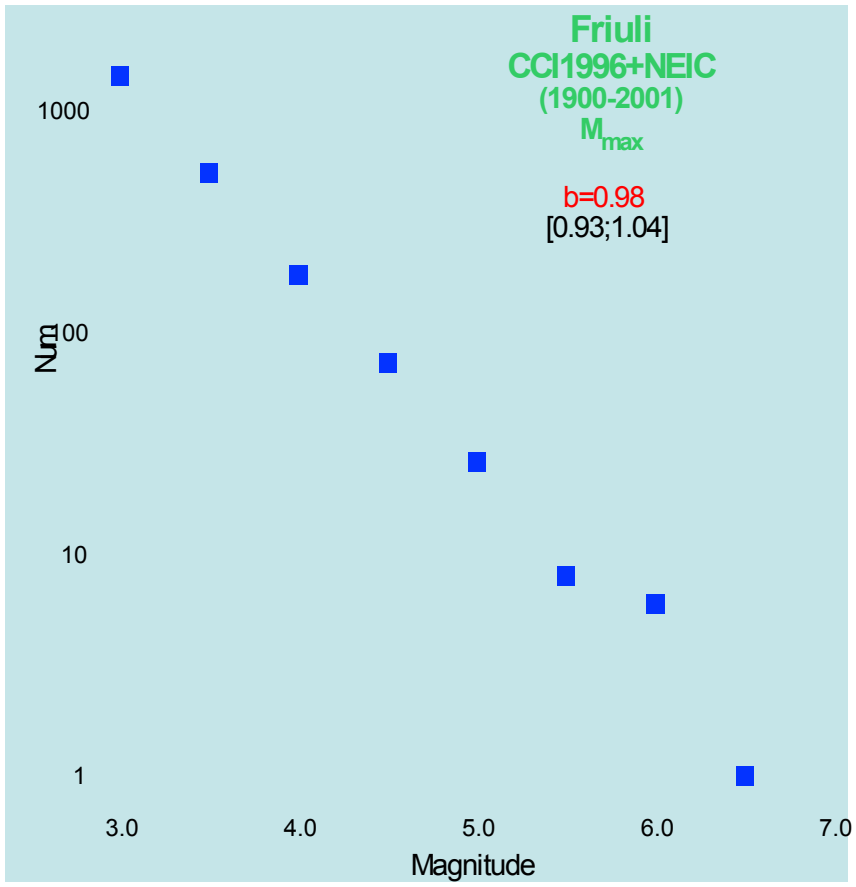

(cumulative distribution)

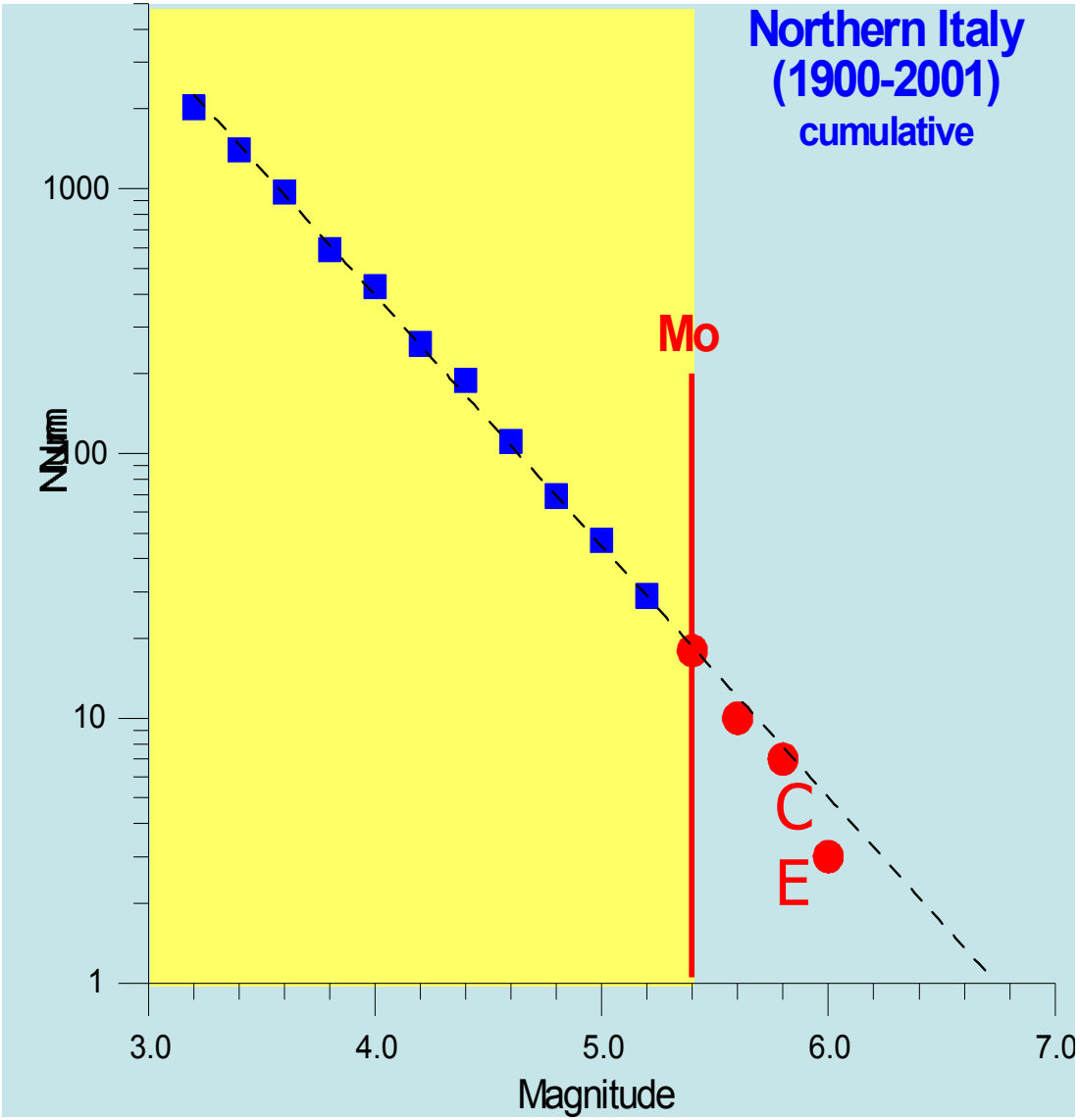

The Gutenberg Richter law when applied to larger (about 500 km in length) regions is linear over the magnitude interval [3-5.4].

The GR law for the entire Italian territory follows a linear trend over the magnitude interval [3-6.7].

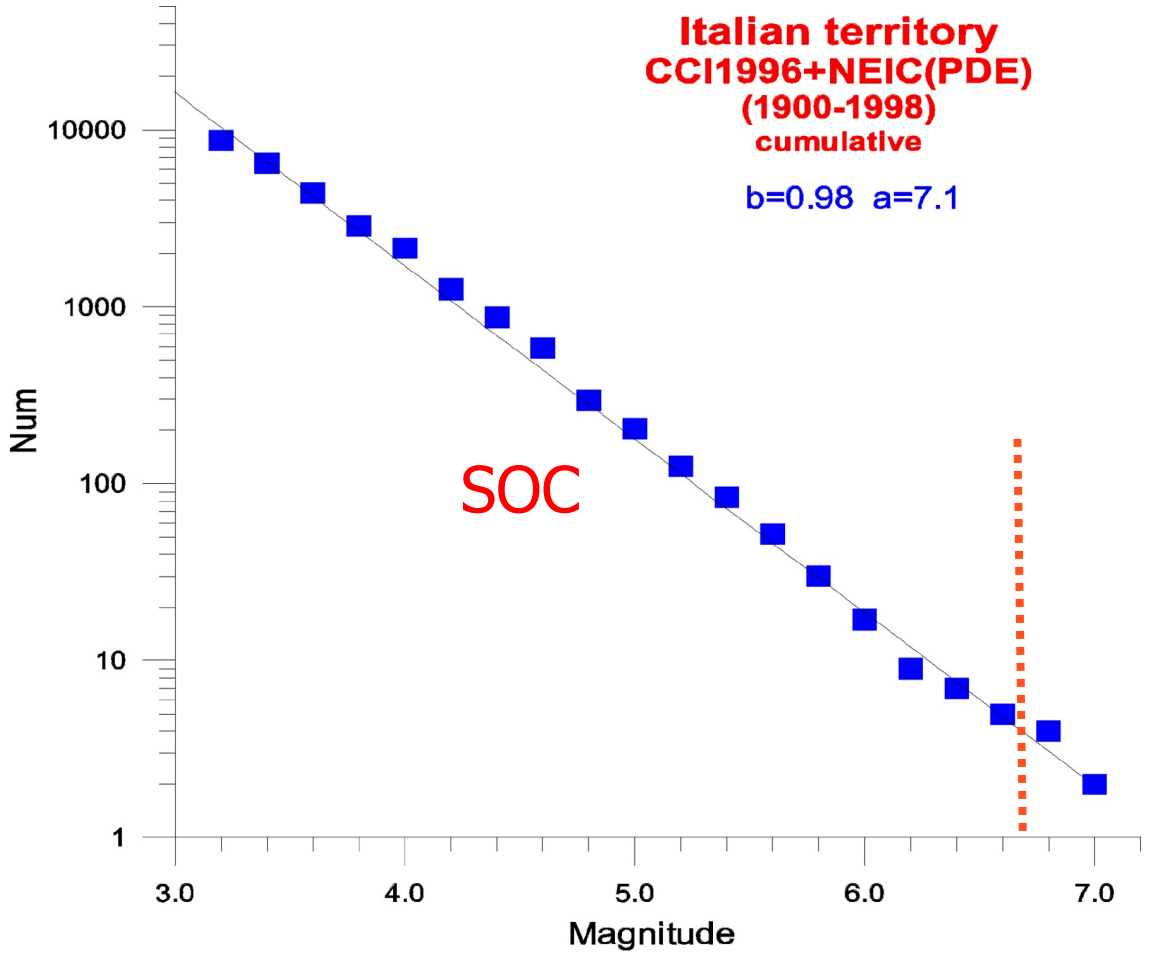

A single GR is not valid for all areas. This fact opens the way to prediction (a SOC system is not predictable) and at the same time casts doubts on the validity of the currently used procedures for the probabilistic assessment of seismic hazard.

Seismic hazard

- The multiscale seismicity model, suggested by *Molchan et al.* (1997) for the purpose of seismic hazard assessment, indicates that:

Seismic hazard

- only the ensemble of events geometrically small, compared with the elements of the seismotectonic regionalization, can be described by a Gutenberg-Richter law;
- therefore the seismic zonation must be performed at several scales with corresponding Gutenberg-Richter laws and magnitude ranges.

? GSHAP ?

Kobe (17.1.1995), Gujarat (26.1.2001), Boumerdes (21.5.2003) Bam (26.12.2003), E-Sichuan (12.5.2008) and Haiti (12.1.2010) earthquakes PGA(g)

	Expected with a probability of exceedence of 10% in 50 years (return period 475 years)	Observed
• Kobe	0.40-0.48	0.7-0.8
• Gujarat	0.16-0.24	0.5-0.6
• Boumerdes	0.08-0.16	0.3-0.4*
• Bam	0.16-0.24	0.7-0.8
• E-Sichuan	0.16-0.24	0.6->0.8
• Haiti	0.08-0.16	0.3-0.6

*from I, if liquefaction is considered the value may be smaller

Global Seismic Hazard Assessment Program (GSHAP) was launched in 1992 by the International Lithosphere Program (ILP) with the support of the International Council of Scientific Unions (ICSU), and endorsed as a demonstration program in the framework of the United Nations Interanational Decade for Natural Disaster Reduction (UN/IDNDR). GSHAP terminated in 1999.

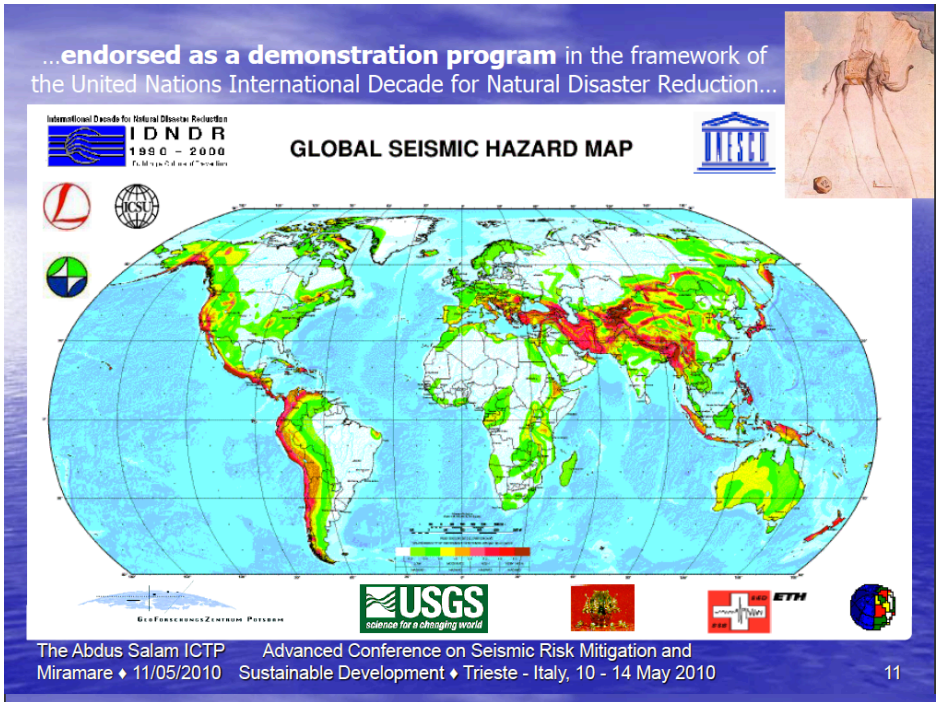

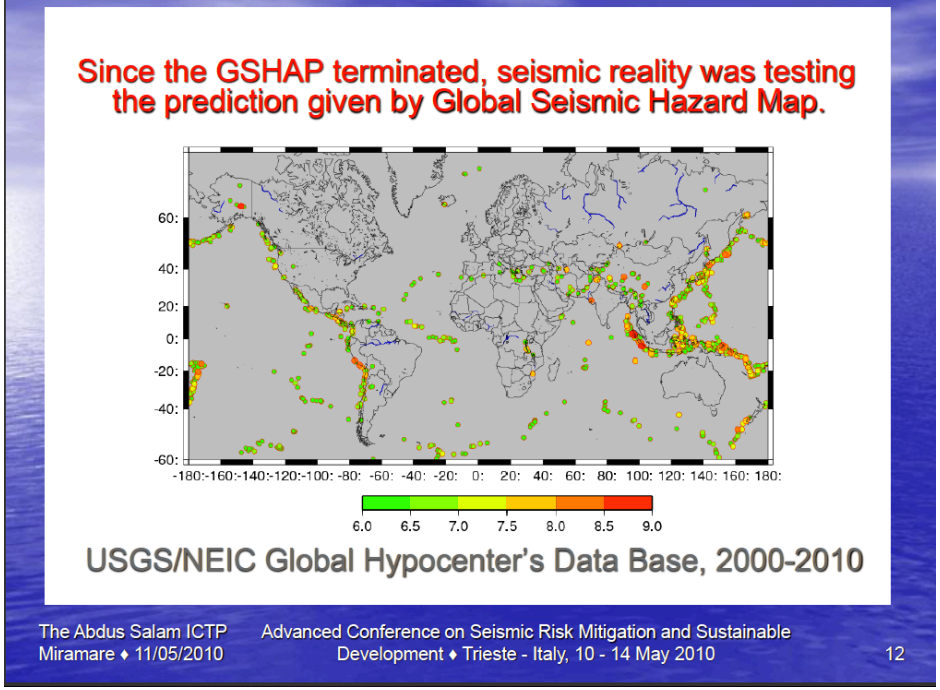

Courtesy

V. Kossobokov,

2010

Each of the 1320 shallow magnitude 6 or larger earthquakes has from 4 to 9 values of the GSHAP PGA at the distance less than 12 km from its epicenter. The maximum of these values is compared to the estimate (*Boore, Joyner and Fumal, 1997*)

$$PGA(M) = EXP(0.53*(M-6)-0.39*LN(10^2+31)+0.25)*9.8$$

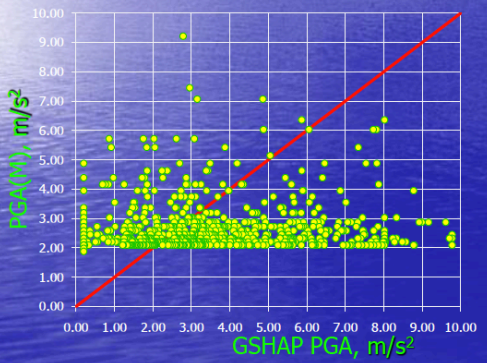

On average the difference is above 1/3 m/s^2; the median equals 1.7 m/s^2

Moreover, 40 out of 56 magnitude 7.5 or larger events have the difference above this average, while for 27 events it is above 2 m/s^2

If we apply transforms to intensity MMI -

$$MMI(M) = 1.5\ (M - 1)$$ (Gutenberg, Richter, 1954)

$$MMI(PGA) = 1.27\ Ln(PGA) - 3.74$$ (Shteinberg et al. 1993)

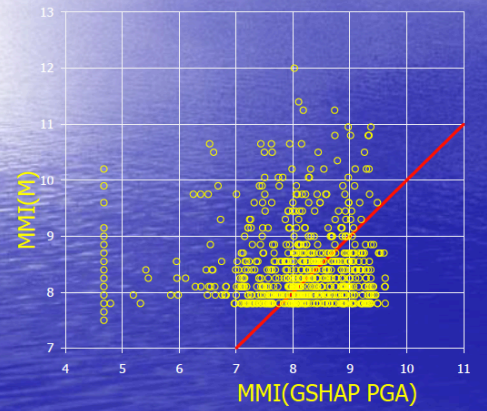

On average the difference is above 1.6; the median equals 2.5.

Moreover, 51 out of 56 magnitude 7.5 or larger events the difference is above 1, while for 30 of those it is above 2

Courtesy

V. Kossobokov,

2010

The Abdus Salam
International Centre for Theoretical Physics

Advanced Conference on "Seismic Risk Mitigation & Sustainable Development"

10 – 14 May 2010
(Miramare - Trieste, Italy)

The Abdus Salam International Centre for Theoretical Physics (ICTP), in the framework of the PCFVG-ICTP Agreement, funded by the Civil Defence of the Friuli Venezia Giulia Region, and the ASI-SISMA Project, funded by the Italian Space Agency, is organizing under the auspices of the Italian Ministry for Environment and Land and Sea (Ministero dell'Ambiente e della Tutela del Mare e del Territorio) an Advanced Conference on "Seismic Risk Mitigation and Sustainable Development". The Conference, co-sponsored by UNESCO-IPRED, GLIS (Working Group on Seismic Isolation), ASSISi (Anti-Seismic Systems International Society) and ENEA, will take place from 10 to 14 May 2010.

The Conference will span from theoretical issues to practical engineering and decision-making problems, recognizing the societal need for a critical and realistic view to earthquake hazard assessment, which should be attained by advanced independent approaches and exploiting of available seismological, geological and geophysical knowledge, to the maximum possible extent.

Top scientists/experts in the field and participants from developing countries (seismologists, engineers, decision makers) are foreseen to attend the Conference. The Conference will facilitate and accelerate interaction of science - practice and exploitation of scientific achievements in the decision-making process. Lectures will cover the following topics:

- *The concept of sustainable development related to Earthquake Preparedness. Hazard and Risk mitigation;*
- *General issues of Seismic Hazard Assessment (SHA). Classical (deterministic and probabilistic) and innovative (neo-deterministic and scenario-based) SHA approaches: advantages and disadvantages. SHA concerns related to seismic regulations;*
- *Advanced SHA tools. Definition of scenario earthquakes. Earthquake lesson and preparedness experience with respect to recent strong earthquakes;*
- *Seismic wave propagation modeling and modeling validation. Strong ground motion data bases and strong motion processing related to the necessity of seismic input modeling;*
- *Seismic zonation at regional, national and metropolitan scale: case studies in Europe, Asia and North Africa;*
- *Educational aspects and problems concerning SHA.*

An open panel discussion will be promoted to debate the limits of current methodologies and available advanced alternatives, taking into account comments and specific requirements from end-users (engineers and stakeholders). The latter will have the possibility of exposure with the most advanced techniques (especially useful in countries which need to start from the very beginning) and will be able to discuss their own situation/problems. The Conference will thus provide a unique opportunity to establish contacts and receive hints for future implementation of the most advanced techniques in developing countries.

Participants are encouraged to make poster presentations illustrating their own recent research and practical problems, related to the Conference issues.

PARTICIPATION

Scientists and students from all countries that are members of the United Nations, UNESCO or IAEA may attend the Conference that will be conducted in English, therefore participants should have an adequate working knowledge of that language.

As a rule, travel and subsistence expenses of the participants should be borne by the home institution. Every effort should be made by candidates to secure support for their fare (or at least half-fare). However, limited funds are available for some participants who are nationals of, and working in, a developing country, and who are not more than 45 years old. Such support is available only for those who attend the entire activity. There is no registration fee.

REQUEST FOR PARTICIPATION

The application form can be accessed at the activity website **http://agenda.ictp.it/smr.php?2142**
Once in the website, comprehensive instructions will guide you step-by-step, on how to fill out and submit the application form.

ACTIVITY SECRETARIAT: ***Telephone:*** **+39-040-2240-355** ***Telefax:*** **+39-040-2240-585**

E-mail: **smr2142@ictp.it** ***ICTP Home Page:*** **http://www.ictp.it/**

October 2009

DIRECTORS

Antonella Peresan
(University of Trieste/ ICTP, Italy)

Mihaela Kouteva
(CLSMEE-BAS, Bulgaria)

Renata Dmowska
(Harvard University, USA)

Badaoui Rouhban
(UNESCO)

LOCAL ORGANIZER

Giuliano F. Panza
(University of Trieste/ ICTP, Italy)

INVITED LECTURERS

Guglielmo Berlasso (Civil Defence FVG, Italy)
Julian Bommer (Imperial College, London, UK)
Luis D. Decanini (La Sapienza U., Rome, Italy)
Rodolfo Guzzi (ASI, Italy)
Jens-Uwe Klügel (NPP Goesgen, Switzerland)
Vladimir Kossobokov (IIEPT-RAS, Russia)
Takashi Imamura (UNESCO–IPRED)
Kojiro Irikura (Kyoto Univ., Japan)
Efraim Laor (Haifa Univ., Israel)
Arthur Lerner-Lam (Columbia Univ., USA)
Norio Okada (DPRI, Kyoto Univ., Japan)
Alessandro Martelli (ENEA and GLIS, Italy)
Michael Melkumyan (ERC, Armenia)
Lalliana Mualchin (Cal.Transp.D. - ret., USA)
James R. Rice (Harvard Univ., USA)
Fabio Romanelli (Trieste Univ., Italy)
Horea Sandi (Acad. Tech. Sci., Romania)
Rodolfo Saragoni (Chile Univ., Chile)
Leonello Serva (ISPRA, Italy)
Dario Slejko (OGS, Italy)
Koji Uenishi (Kobe Univ., Japan)
Franco Vaccari (Trieste Univ., Italy)
Peter Varga (CEI and GGRI, Hungary)
Zhenming Wang (Kentucky Univ., USA)
Zhongliang Wu (CEA, China)

Deadline for requesting participation:

10 January 2010

Pure and Applied Geophysics Topical volume 2010

Advanced Seismic Hazard Assessment

Editors: *G.F. Panza (Italy), K. Irikura (Japan), M. Kouteva (Bulgaria), A. Peresan (Italy), Z. Wang (USA), R. Saragoni (Chile)*

Intermediate-term Intermediate-range earthquake prediction

Uncertainty:

Time: a few years

Space: a few hundreds kilometres

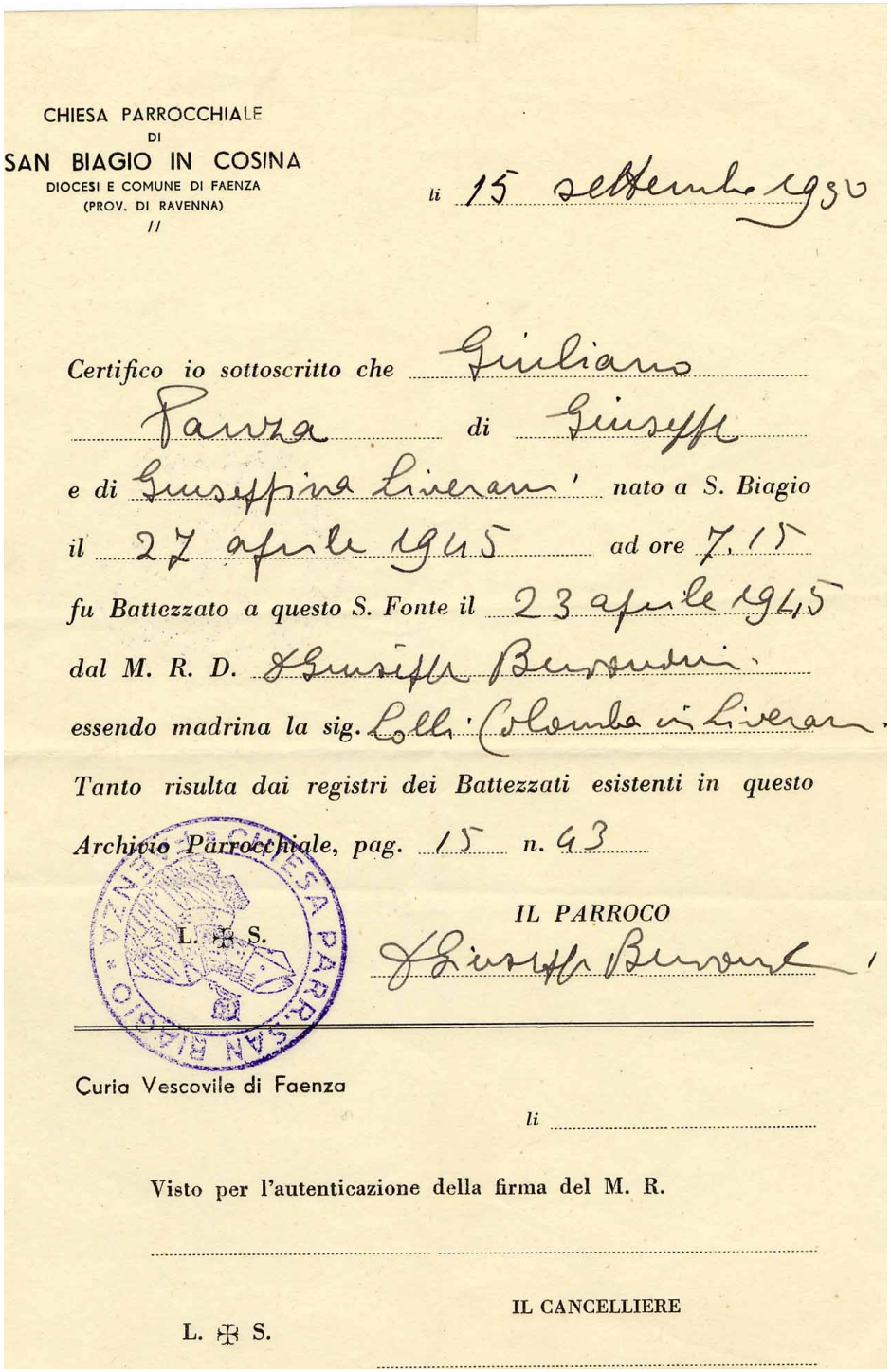

CHIESA PARROCCHIALE
DI
SAN BIAGIO IN COSINA
DIOCESI E COMUNE DI FAENZA
(PROV. DI RAVENNA)
//

li 15 settembre 1950

Certifico io sottoscritto che Giuliano
Pavza *di* Giuseppe
e di Giuseppina Liverani *nato a S. Biagio*
il 27 aprile 1945 *ad ore* 7.15
fu Battezzato a questo S. Fonte il 23 aprile 1945
dal M. R. D. Giuseppe Bersani
essendo madrina la sig. Lolli Colomba in Liverani
Tanto risulta dai registri dei Battezzati esistenti in questo
Archivio Parrocchiale, pag. 15 *n.* 43

L. ✠ S.

IL PARROCO
Giuseppe Bersani

Curia Vescovile di Faenza

li .....

Visto per l'autenticazione della firma del M. R.

IL CANCELLIERE

L. ✠ S.

My earliest credential about prediction

This is my certificate of baptism, drafted on September 15, 1950, stating that I was **born** on April **27**, 1945 and I was **christened** on April **23**,1945

Intermediate-term earthquake prediction

- A family of intermediate-term earthquake prediction algorithms has been developed on the basis of the understanding that the seismically active lithosphere has to be regarded as a hierarchical non-linear (chaotic) dissipative system, as well as by the application of pattern recognition techniques.

- **In agreement with the Multiscale approach, inside the monitored regions, the linearity of the GR is preserved only for magnitudes not larger than M_o**

- **Prediction Algorithms (CN and M8) are based on the formal analysis of the anomalies in the flow of the seismic events that follow the GR law, and predict the strong events ($M>M_0$) that are rare and do not follow GR inside the delimited region**

Intermediate-term earthquake prediction

- The high statistical significance of this kind of prediction was established on the basis of prediction of strong earthquakes in numerous regions world-wide, 1985 - 2001.
- Prediction is reproducible; complete formal definition of the algorithms was published in advance.

Real-time monitoring of the seismic flow

Italy: real time earthquake prediction experiment started in July 2003 (*Peresan al., Earth Sci. Rev. 2005*).

Algorithms fully formalized and globally tested for intermediate-term middle-range earthquake prediction are:

- **CN algorithm** (***Gabrielov et al., 1986; Rotwain and Novikova, 1999***)
- **M8S algorithm** (***Keilis-Borok and Kossobokov, 1987; Kossobokov et al., 2002***)

Updated predictions are regularly posted at:

www.ictp.trieste.it/www_users/sand/prediction/prediction.htm

Current predictions are accessible via password only, to prevent improper use of research on earthquake prediction but to permit rigorous *real time* test of the used methodologies

- **Predictions for Italy are performed for three different magnitude ranges, namely M6.5+, M6.0+ and M5.5+ where M_0+ indicates the magnitude range: $M_0 \leq M \leq M_0+0.5$.**

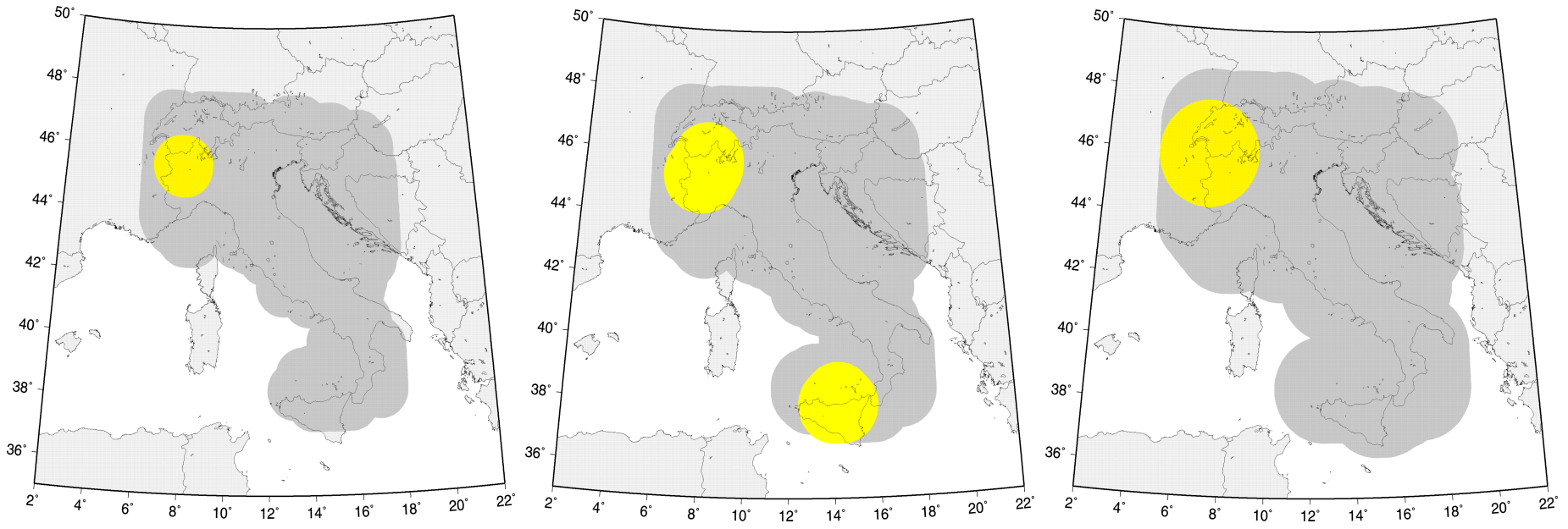

Space-time volume of alarm in M8S application in Italy

Experiment	M6.5+		M6.0+		M5.5+	
	Space-time volume, %	n/N	Space-time volume, %	n/N	Space-time volume, %	n/N
Retrospective (1972-2001)	36	2/2	40	1/2	39	9/14
Forward (2002-2010)	35	0/0	39	0/1	20	5/9
All together (1972-2010)	36	2/2	40		35	14/23

Algorithm M8s predicted 60% of the events occurred in the monitored zones in Italy, i.e. 17 out of 28 events occurred within the area alerted for the corresponding magnitude range. The confidence level of M5.5+ predictions since 1972 has been estimated to be above 98%; no estimation is yet possible for other magnitude levels.

(updated to July 1 2010;
next updating January 1 2011)

A complete archive of M8S predictions in Italy can be view
http://www.ictp.trieste.it/www_users/sand/prediction/prediction.htm
http://www.mitp.ru/prediction.htm

The M8S real-time monitoring of seismic flow

Real-time testing M5.5+, 2002-2010

Date	Latitude, ^{0}N	Longitude, ^{0}E	Depth, êì	M_{max}	M8S	Location
2002.09.06	38.38	13.70	5	5.9	No	Near Sicily
2002.10.31	41.79	14.87	10	5.9	No	South Italy
2003.03.29	43.11	15.46	10	5.5	Yes	Adriatic sea
2003.09.14	44.33	11.45	10	5.6	Yes	Near Bologna
2004.02.23	47.27	6.27	17	5.5	Yes	Switzerland
2004.05.05	38.51	14.82	228	5.5	No	Near Sicily
2004.07.12	46.30	13.64	24	5.6	No	Slovenia
2004.11.24	45.63	10.57	24	5.5	Yes	North Italy
2006.10.26	38.67	15.40	216	5.8	Yes	Near Sicily

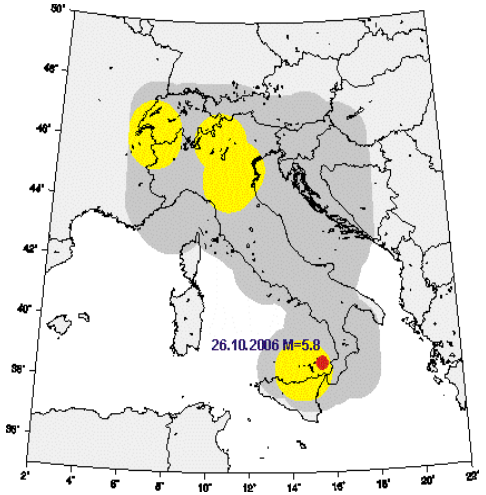

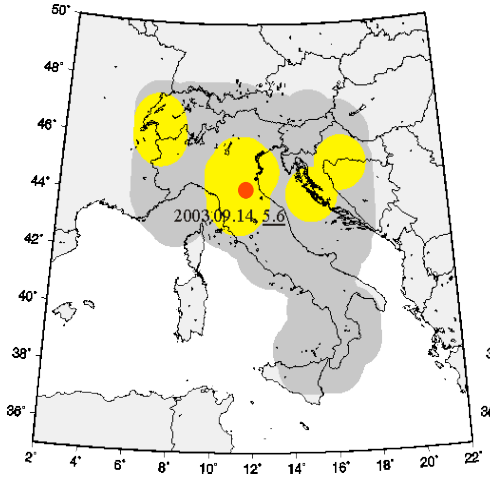

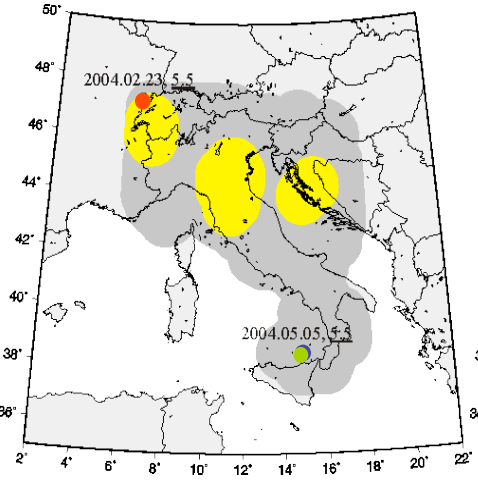

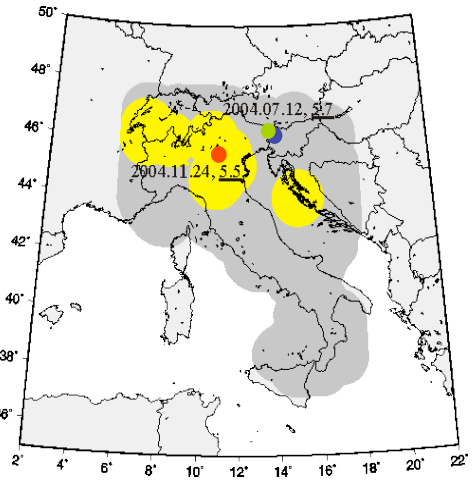

Monitored region

Alerted region

Events with M_{max} ≥5.5 occurred since July 2003

Updated to July 1 2010

- **The algorithm CN analyses the seismic activity inside a set of predefined polygons (regions), outlined strictly following the seismotectonic zoning** (*Peresan, Costa & Panza., 1999, Pageoph, 154*)

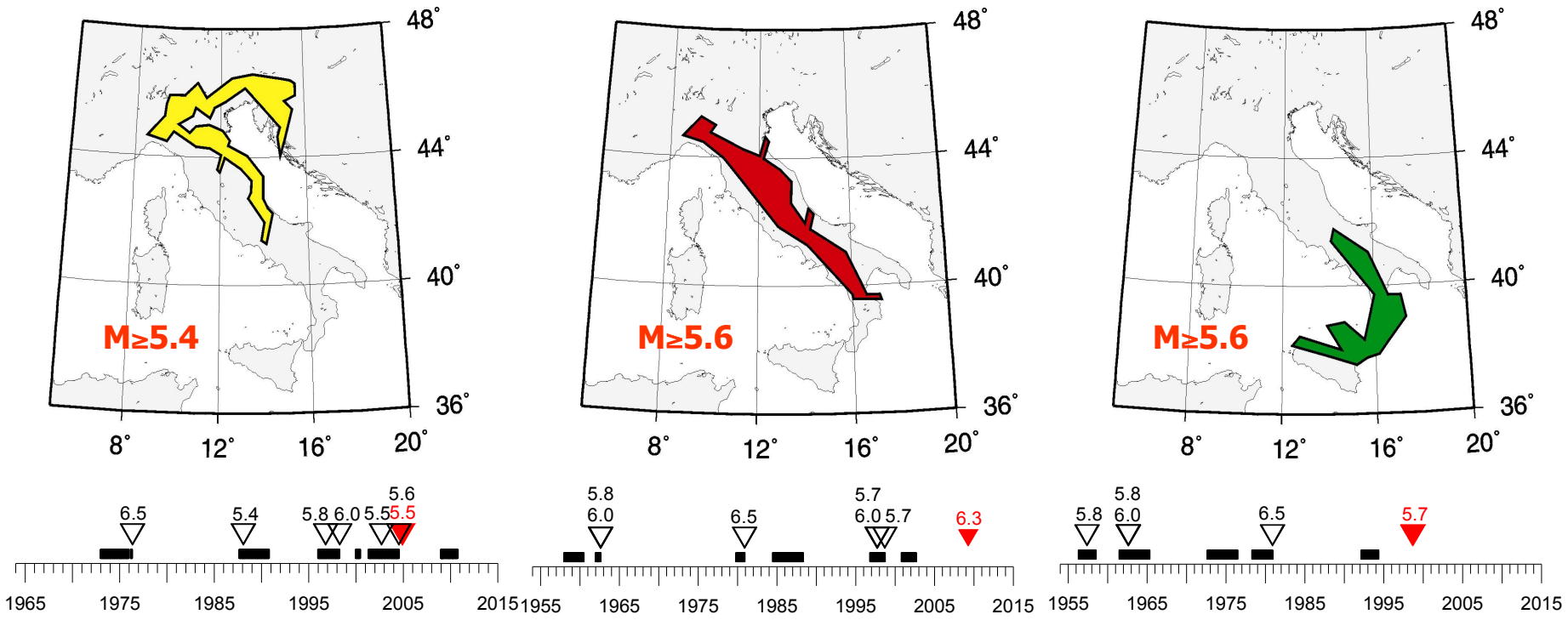

Space-time volume of alarm in CN application in Italy

Experiment	Space-time volume of alarm (%)	n/N	Confidence level (%)
Retrospective* (1954 – 1963)	41	3/3	93
Retrospective (1964 – 1997)	27	5/5	>99
Forward (1998 – 2010)	27	4/6	95
All together (1954 – 2010)	29	12/14	>99

* Central and Southern regions only

Algorithm CN predicted 12 out of the 14 strong earthquakes occurred in the monitored zones of Italy, with less than 30% of the considered space-time volume occupied by alarms.

(updated to September 1 2010;
next updating November 1 2010)

A complete archive of CN predictions in Italy can be viewed at:
http://www.ictp.trieste.it/www_users/sand/prediction/prediction.htm

e-mail: aperesan@units.it I

The CN real-time monitoring of seismic flow

Real-time testing 1998-2010

Earthquakes occurred within the space-time-magnitude volume monitored by CN since 1998

Date	Latitude, ^{0}N	Longitude, ^{0}E	Depth, km	M	CN	Location
1998.04.12	46.24	13.65	10	6.0	Yes	Slovenia
1998.09.09	40.03	15.98	10	5.7	Yes	South Italy
2003.09.14	44.33	11.45	10	5.5	Yes	Near Bologna
2004.07.12	46.30	13.64	24	5.6	Yes	Slovenia
2004.11.24	45.63	10.57	24	5.5	No	North Italy
2009.04.06	42.33	13.33	9	6.3	No	Central Italy

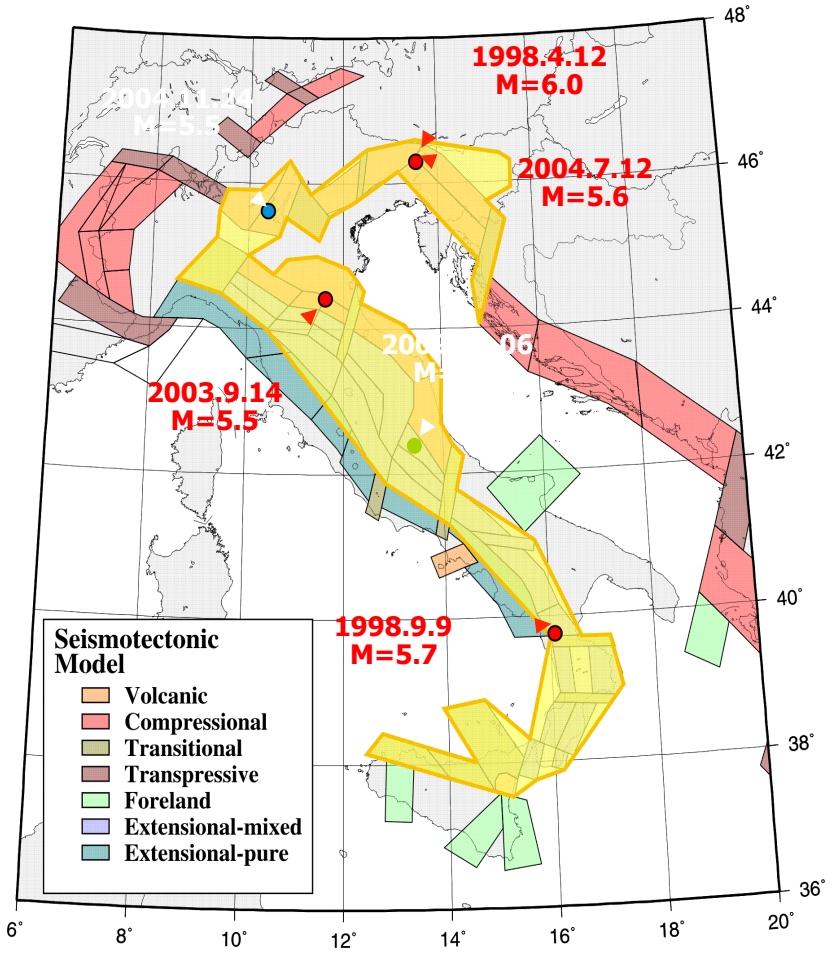

Updated to May 1 2010 (next updating July 1 2010)

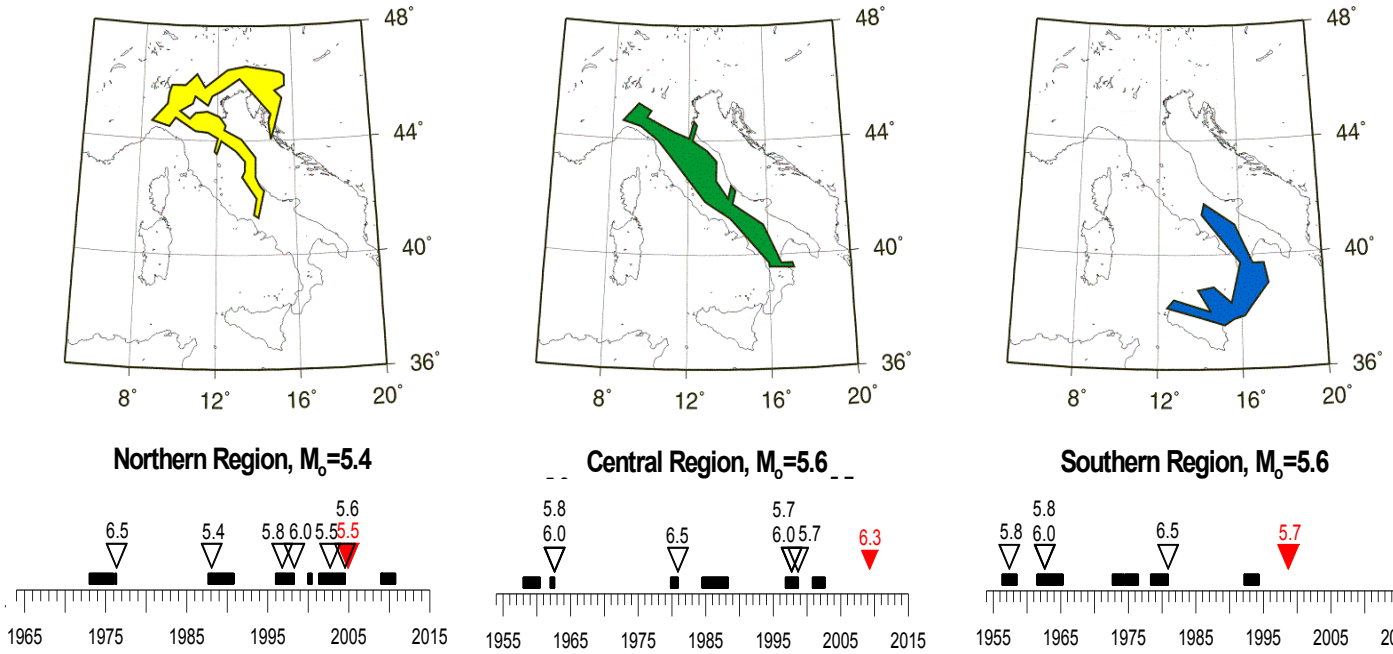

CN algorithm

Times of Increased Probability for the occurrence of events with M>Mo within the monitored regions

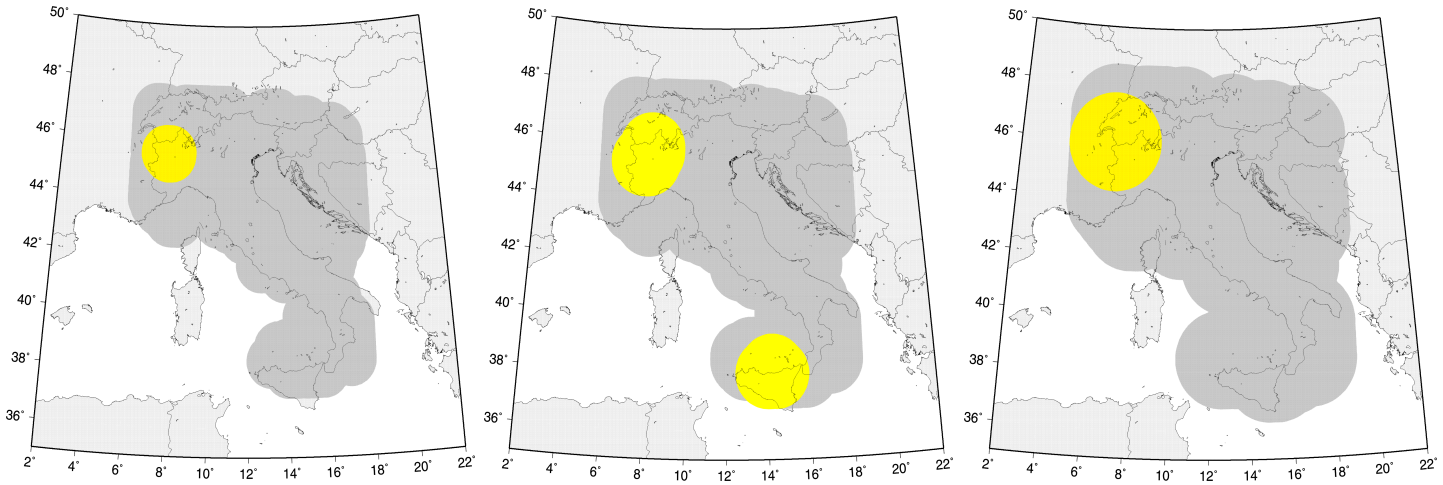

M8S algorithm

Monitored region

Alerted region

M5.5+ **M6.0+** **M6.5+**

(*Peresan al., Earth Sci. Rev. 2005*)

Intermediate-term middle-range earthquake prediction

Evaluation of prediction results

The quality of prediction results can be characterised by using two prediction parameters (*Molchan, 1997*) **:**

η **: the rate of failures-to-predict (*n/N*)**

τ **: the space-time volume of alarm**

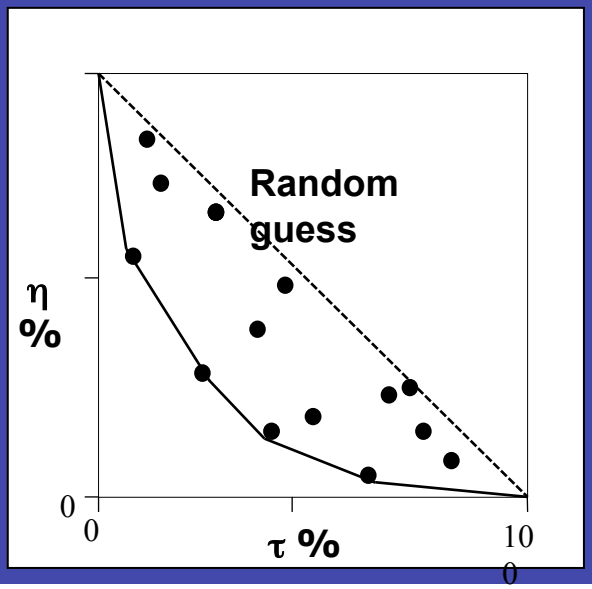

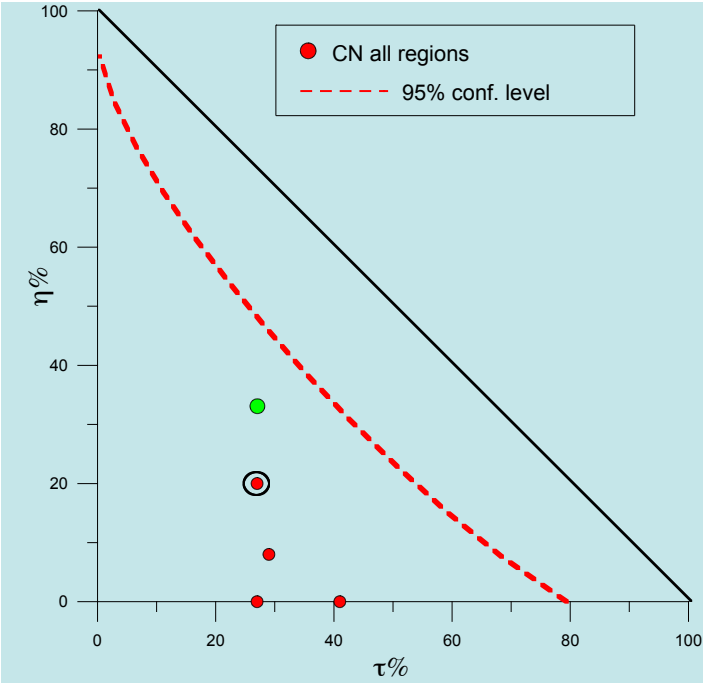

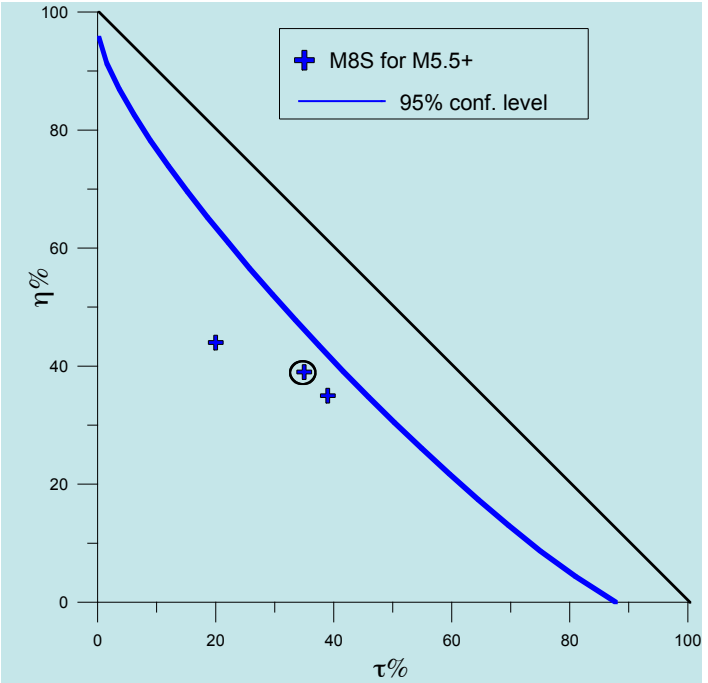

CN and M8S predictions in Italy

(Scores as on January 1 2010)

Intermediate-term Intermediate-range earthquake prediction and Earth Observations

Integration with geodetic observations

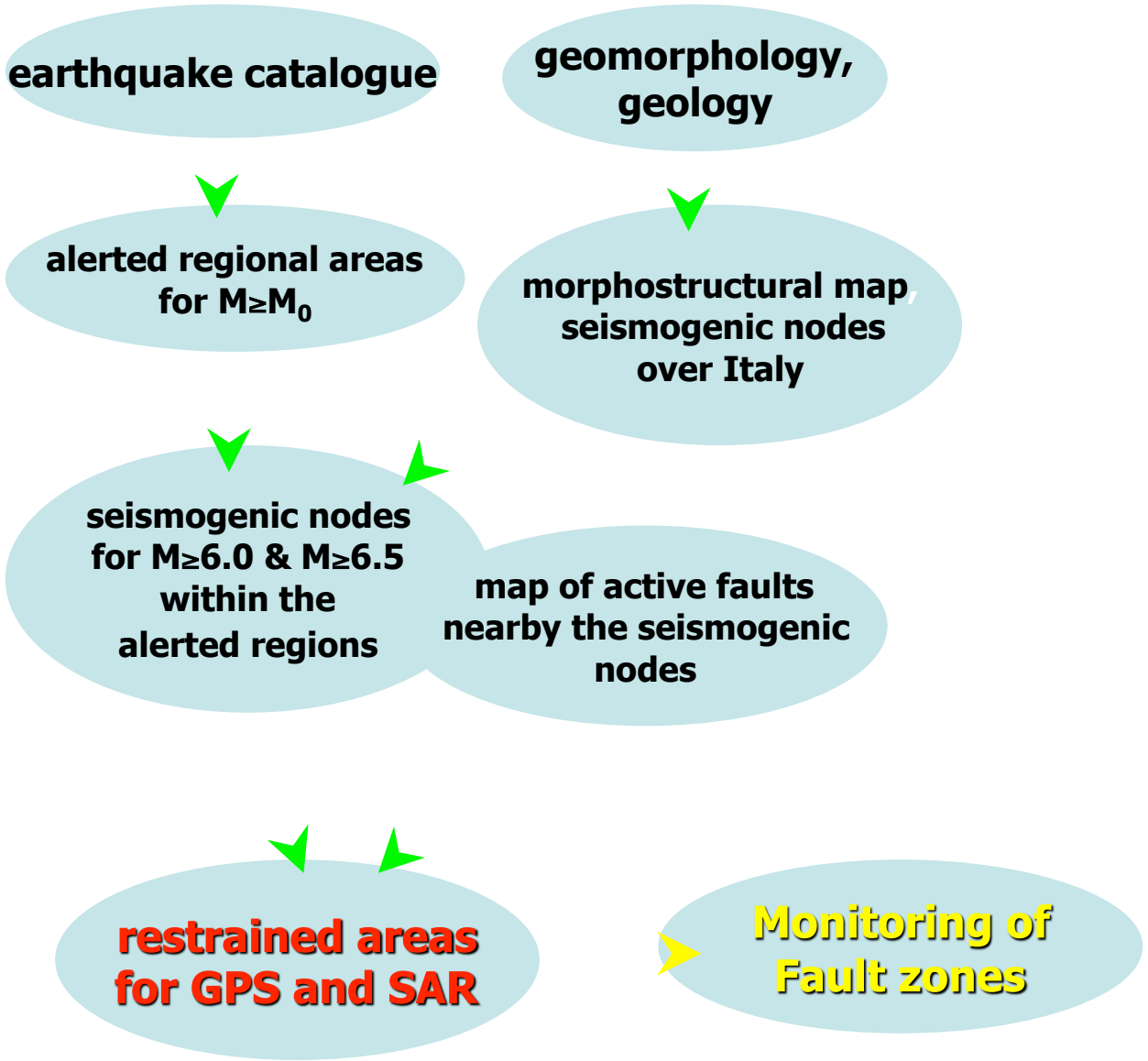

ASI Pilot Project - SISMA
"Seismic Information System for Monitoring and Alert"

Development of a system, based on the neo-deterministic approach for the estimation of seismic ground motion, integrating the space and time dependent information provided by real-time monitoring of seismic flow and EO data analysis, through geophysical forward modeling.

agenzia spaziale italiana

DST

University of Milano

Politecnico di Milano

galileian PLUS

L’Aquila 6 April 2009
M_w=6.3 event

Prediction of subsequent strong earthquake after Aquilano earthquake, April, 6, 2009, Mw=6.3

Subsequent strong earthquake with magnitude M>=5.3 is expected till October, 6, 2010 within 43Km of Aquilano earthquake epicenter

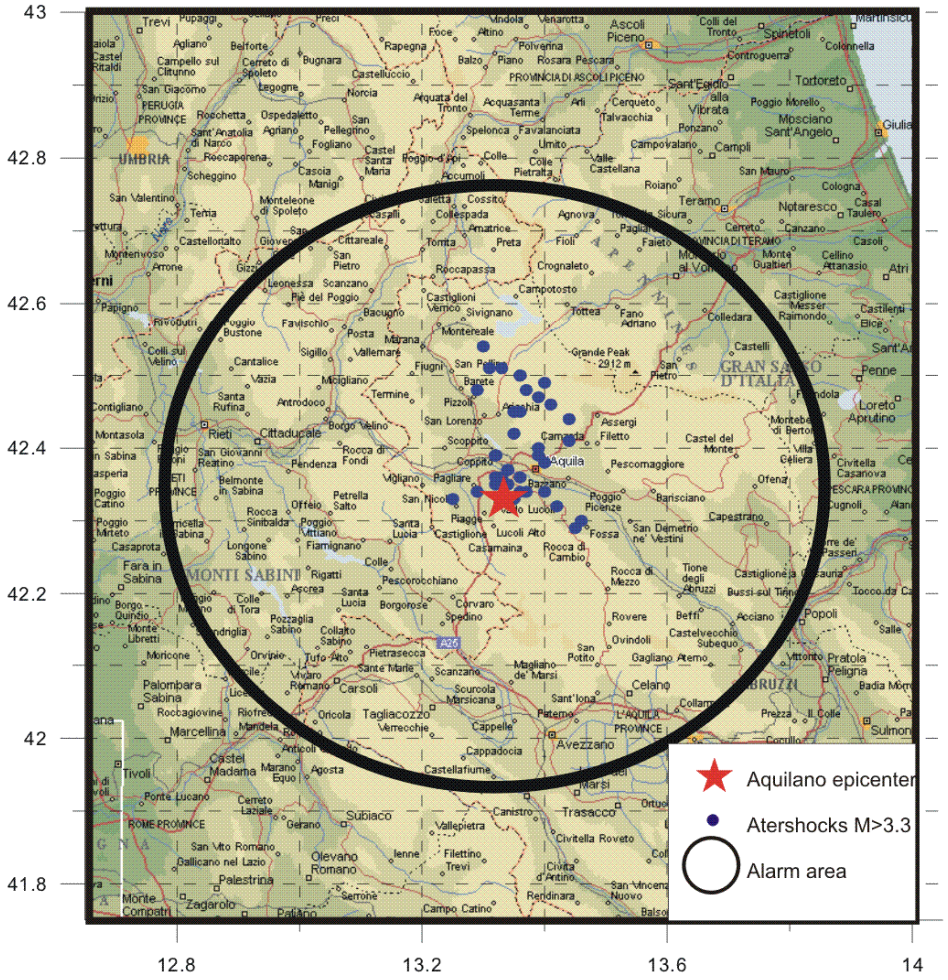

Prediction formulated April 25, 2009 with SSE algorithm (Vorobieva, I.A. (1999) Prediction of the subsequent large earthquake. *Phys. Earth and Planet. Inter.*, **111**, 3-4: 197-206; and Vorobieva,I.A., and G.F.Panza, Prediction of the occurrence of related strong earthquakes in Italy. *PAGEOPH*, 1993, 141, 1: 25-41.

Advanced post-seismic deformation analysis

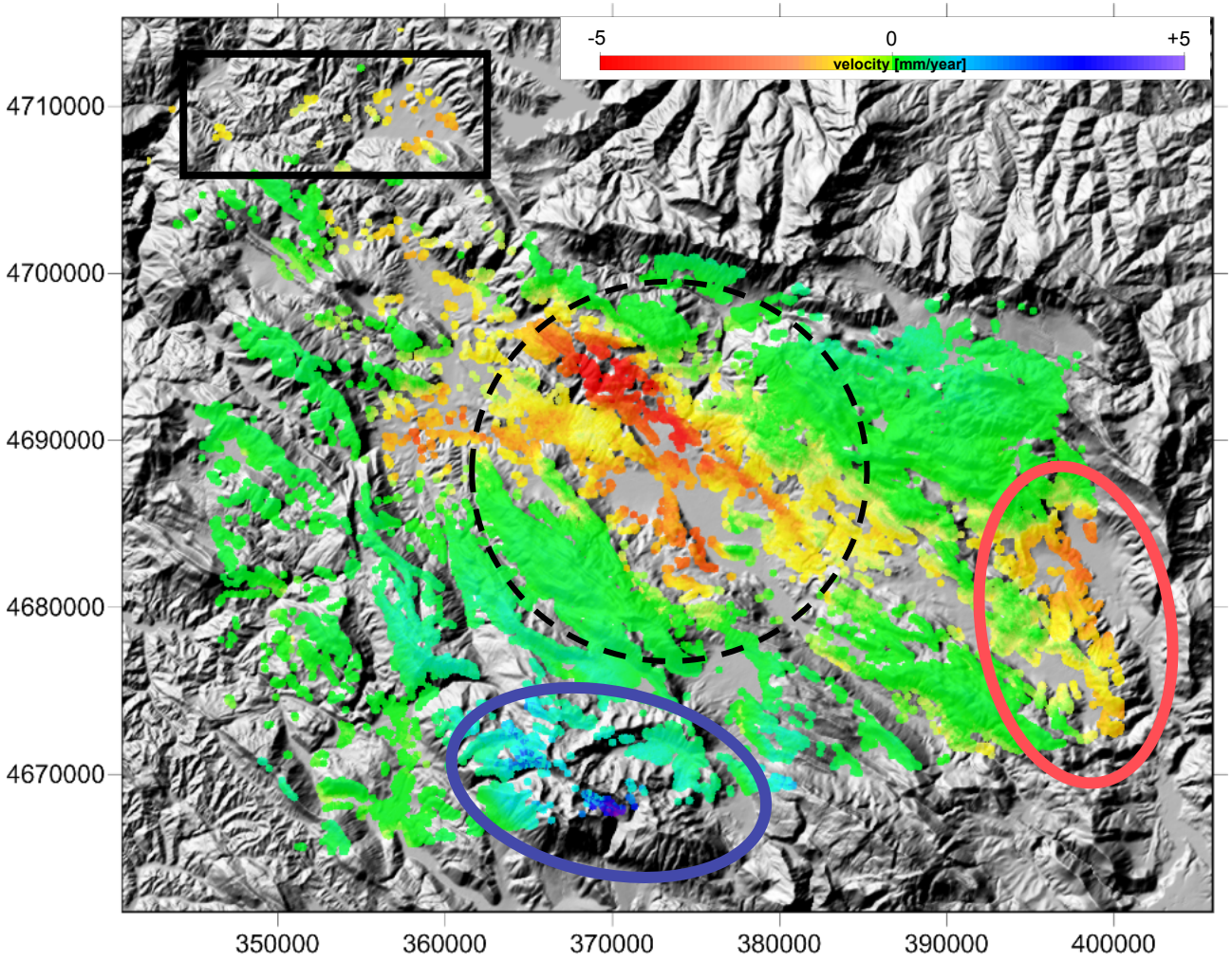

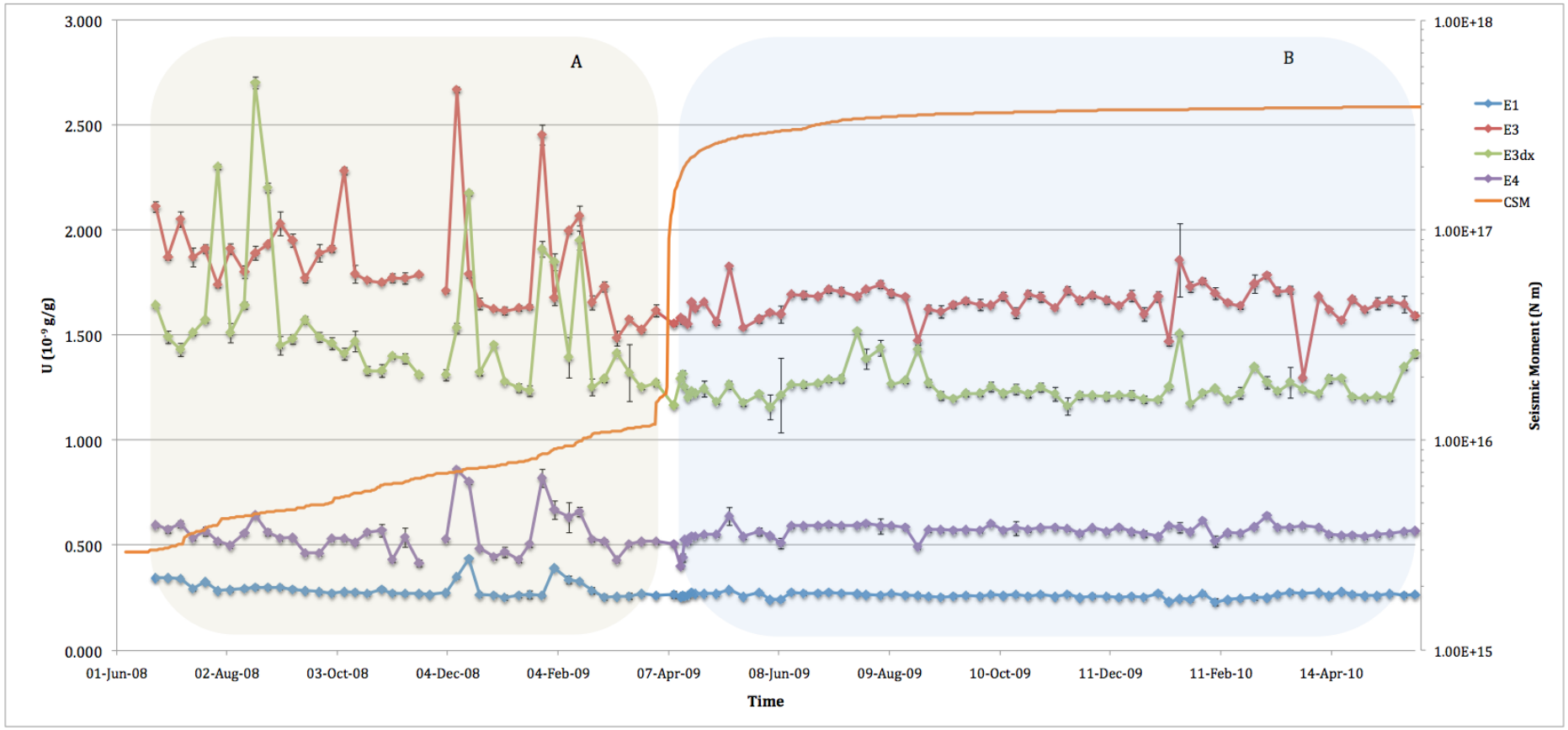

Time variation of U concentration in groundwater sampled in 4 sites at INFN Gran Sasso National Laboratory from June 2008 to May 2010. In the period A, from 23rd June 2008 to 31st March 2009, these readings show a clear short-term 40-80% peak structure. In the period B, from 10th April 2009 to 31st May 2010, a peak structure for U is visible again after September 10, 2009.

The cumulative seismic moment (CSM) from January 2008 to May 2010 in the area 42.00°-42.75°N and 12.75°-13.75°E has been estimated from seismic data of the Italian Seismic Bulletin, INGV: the clear jump in the CSM coincides with the main shock on April, 6th, 2009. (Plastino et al., in preparation, ICTP preprint)

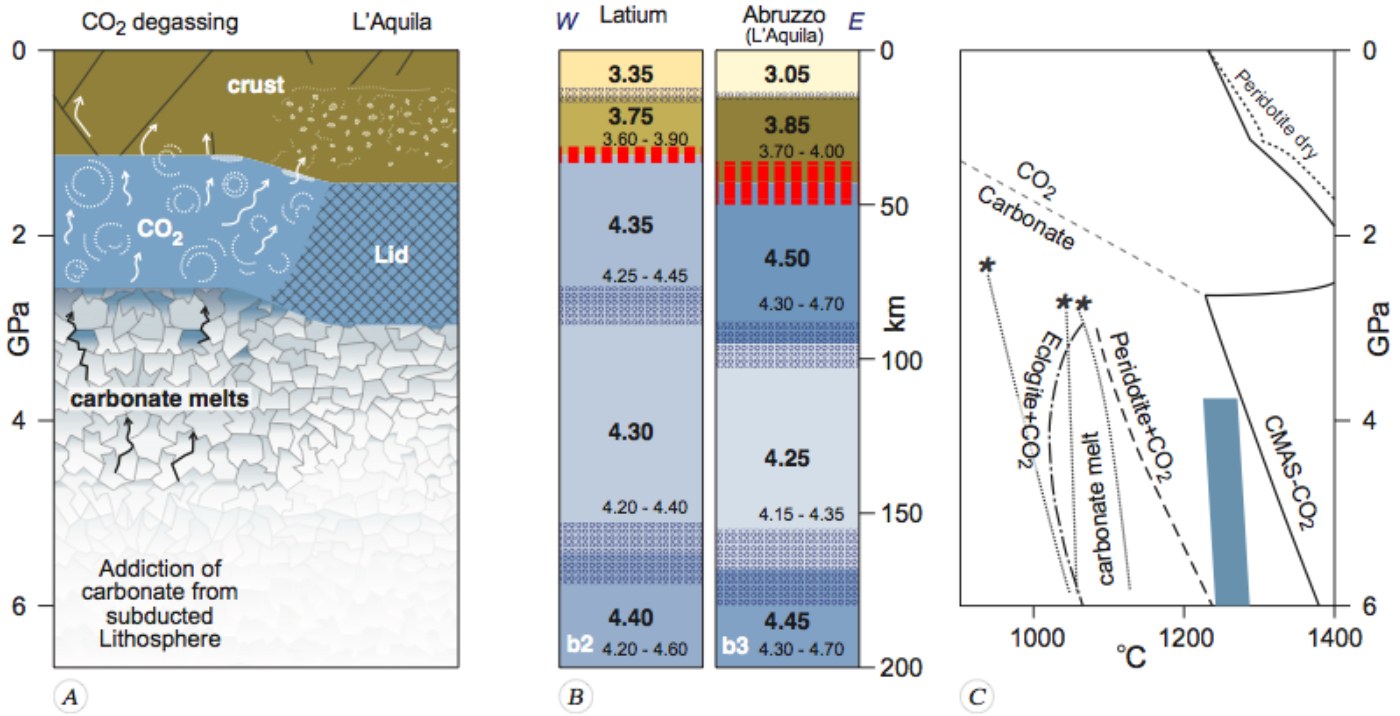

Present-day architecture of mantle-CO_2 degassing beneath L'Aquila (Central Italy). The generation and evolution of deep mantle-derived CO_2 (A) has been delineated integrating surface wave tomography (B) with experimentally determined melting relationships for carbonated peridotite and crustal lithologies, relevant to recent mantle processes in the western Mediterranean region (C). (A) Geochemical reconstruction (0-200 km depth) beneath the Latium – Abruzzo (L'Aquila) region (Central Italy). (B) Models of shear-wave velocities (km s^{-1}) vs depth for Latium and Abruzzo (L'Aquila) zones; the shadowed areas indicate the range of variability of the thickness of the layers, the red dashed lines mark the range of variability of the Moho depth; this representation is used to evidence that the boundaries between layers can well be transition zones in their own right. (C) Pressure-temperature diagram showing the effects of CO_2 on upper mantle lithologies. Peridotite - CO_2 solidus; Peridotite - CO_2 and Dry Peridotite solidi in the CMSA system; Eclogite - CO_2 solidus. KNCFMASH - CO_2 solidus (carbonated pelite + 1.1 wt.% H_2O + 4.8 wt.% CO_2). Blue area = estimated standard present-day mantle temperatures at the inferred pressures. Melting of sediments and/or continental crust of the subducted Adriatic lithosphere at pressures greater than 4 GPa (120 km) and temperatures of 1200 −C (C – blue area) generate carbonate-rich melts. Such melts, migrating upward through the mantle, form a carbonated partially molten layer recorded by tomographic images between 70 and 160 km of depth (B – cell b2). Further upwelling of carbonate-rich melts induces massive outgassing of CO_2 in the lithospheric mantle (C – carbonate – CO_2 field boundary). High velocities in the uppermost mantle beneath Abruzzo (L'Aquila) support evidence for a LID initiating to subduct toward the west. Beneath Latium, at the same depth, an asthenospheric mantle wedge is present, as indicated by the quite low V_s between 40 and 80 km of depth (LID; B – cell b3). (Plastino et al., in preparation, ICTP preprint).

Thanks to **Mentors** and Co-workers:

Stephan Mueller

Leon Knopoff

Volodya Keilis-Borok*

Tolya Levshin*

Carlo Doglioni

Angelo Peccerillo

Roberto Sabadini

*Alik Ismail-Zadeh**

*Volodya Kossobokov**

*Antonella Peresan**

*Reneta Raykova**

*Fabio Romanelli**

Gildo Calcagnile

Karim Aoudia

Eugenio Carminati

**SAND*

References

Ampferer, O., 1906. Uber das Bewegungbild von Faltengebirge, Austria. Geol. Bundesanst. Jahrb., 56, 539-622.

Chiarabba, C., et al., 2008. The southern Tyrrhenian subduction zone: Deep geometry, magmatism and Plio-Pleistocene evolution. Earth and Planetary Science Letters, 268, 408-423.

Baccheschi, P., Margheriti, L. and Steckler, M. S. (2007). Seismic anisotropy reveals focused mantle flow around the Calabrian slab (Southern Italy), G.R.L., 34, L05302, doi:10.1029/2006GL028899.

Boyadzhiev, G., Brandmayr, E., Pinat, T. and Panza, G.F., 2008. Optimization for non-linear inverse problems. Rendiconti Lincei, 19, 17-43.

Brandmayr, E., Raykova, R., Zuri, M., Romanelli, F., Doglioni, C., and Panza, G., 2010. The lithosphere in Italy: structure and seismicity. In: Beltrando, M., Peccerillo, A., Mattei, M., Conticelli, S. and Doglioni, C. (Eds.), Journal of the Virtual Explorer, volume 36, paper 1, doi: 10.3809/jvirtex.2009.00224

Chimera, G., Aoudia, A., Saraoɔ, A. and Panza, G.F., (2003). Active tectonics in Central Italy: constraints from surface wave tomography and source moment tensor inversion. PEPI, 138, 241- 262.

Doglioni C., Green D. and Mongelli F. (2005): On the shallow origin of hotspots and the westward drift of the lithosphere: in Plates, Plumes and Paradigms, G.R. Foulger, J.H. Natland, D.C. Presnall, & D.L. Anderson (Eds), GSA Sp. Paper 388, 735-749.

Doglioni C., Carminati E., Cuffaro M. and Scrocca D. (2007): Subduction kinematics and dynamic constraints. Earth Science Reviews, 83, 125-175, doi:10.1016/j.earscirev.2007.04.001.

Frezzotti, M.L., Peccerillo, A. and Panza, G.F., (2009).Carbonate metasomatism and CO2 lithosphere-asthenosphere degassing beneath the Western Mediterranean: An integrated model arising from petrological and geophysical data, Chemical Geology, 262, 108-120.

Ismail-Zadeh, A.T., Aoudia, A., and Panza, G.F., (2004). Tectonic Stress in the Central Apennines due to Lithospheric Buoyancy. Doklady Earth Sciences, 395A, 3, 2004, 369-372.

Ismail-Zadeh, A., Aoudia, A. and Panza, G.F., (2010). Three-dimensional numerical modeling of contemporary mantle flow and tectonic stress beneath the Central Mediterranean, Tectonophysics, 482, 226-236.

Kelly, R.K., Kelemen, P.B., Jull, M., 2003. Buoyancy of the continental upper mantle. G3. 4 (2), 1017.

Mueller, S. and Panza, G.F., (1986). Evidence of a deep-reaching lithospheric root under the Alpine Arc. In: The Origin of Arcs, ed. by: F.C. Wezel, Elsevier, 21, 93-113.

Panza, G.F., Mueller, S., 1978. The plate boundary between Eurasia and Africa in the Alpine Area. Mem. Soc. Geol. It., 33, 43-50.

Panza, G.F., Calcagnile, G., Scandone, P. and Mueller, S., (1980). La struttura profonda dell' Area Mediterranea. Le Scienze, 141, 60-69.

Panza, G.F., Mueller, S., Calcagnile, G. and Knopoff, L., (1982). Delineation of the north central Italian upper mantle anomaly. Nature, 296, 238-239.

Panza, G.F., Doglioni, C. and Levshin, A., (2010). Asymmetric ocean basins, Geology, 38, 1, 59-62.

References

Panza, G. F., Raykova, R. B., Carminati, E., Doglioni, C., (2007). Upper mantle flow in the western Mediterranean. EPSL, 257, 200-214.

Panza, G.F. and Sarao', A., (2000). Monitoring volcanic and geothermal areas by full seismic moment tensor inversion: are non-double-couple components always artefacts of modelling? Geophysical Journal International, 143, 353-364.

Peccerillo, A., 2005. Plio-Quaternary volcanism in Italy. Springer, Heidelberg, 365 pp.

Raykova, R.B. and Panza, G.F., (2006). Surface waves tomography and non-linear inversion in the southeast Carpathians. Physics of the Earth and Planetary Interiors, 157, 164-180

Riguzzi, F., Panza, G., Varga P. and Doglioni, C., (2010). Can Earth's rotation and tidal despinning drive plate tectonics?, Tectonophysics, 484, 60-73.

Saraò, A., Cocina O., Privitera, E. and Panza, G.F., (2010). The dynamics of the 2001 Etna eruption as seen by full moment tensor analysis, Geophys. J. Int., 181, pp. 951-965.

Scalera, G., 2007. A new model of orogenic evolution Rend. Soc. Geol. It., 5, Nuova Serie, 214-218.

Scalera, G., 2005. A new interpretation of the Mediterranean arcs: Mantle wedge intrusion instead of subduction Boll. Soc. Geol.It., Volume Speciale n. 5, 129-147.

Scalera, G., 2008 Great and old earthquakes against great and old paradigms – paradoxes, historical roots, alternative answers. Adv. Geosci., 14, 41–57, 2008

Scoppola B., Boccaletti D., Bevis M., Carminati E. and Doglioni C. (2006): The westward drift of the lithosphere: a rotational drag? Bull. Geol. Soc. Am., 118, 1/2; p. 199–209; doi: 10.1130/B25734.1.

Sileny, J. and Panza, G.F., (1991). Inversion of seismograms to determine simultaneously the moment tensor components and source time function for a point source buried in a horizontally layered medium. Studia Geophysica et Geodaetica, 35, pp. 166-183.

Sileny, J., Panza, G.F. and Campus, P., (1992). Waveform inversion for point source moment tensor retrieval with variable hypocentral depth and structural model. Geophys. J. Int., 109, pp. 259-274.

Spakman, W., Wortel, M. J. R., Vlaar, N. J. (1988):. The Hellenic subduction zone: A tomographic image and its geodynamic implications, G.R.L., 15, 60-63.

Zhang, Yu-Sh. and Tanimoto, T. (1992) Ridges, hotspots and their interaction as observed in seismic velocity maps. Nature, 355, 45 - 49; doi:10.1038/355045a0.